

# Three-dimensional micro- and nanostructural characteristics of the scleractinian coral skeleton: A biocalcification proxy

JAROSŁAW STOLARSKI



Stolarski, J. 2003. Three-dimensional micro- and nanostructural characteristics of the scleractinian coral skeleton: A biocalcification proxy. *Acta Palaeontologica Polonica* 48 (4): 497–530.

The contemporary “two-step model” of growth of the scleractinian skeleton is based mostly on transversely sectioned samples. According to this model, many skeletal elements e.g., septa are formed in two temporally distinct phases represented by (1) “centers of calcification” that are composed of homogeneously distributed microcrystalline or/and organic components and serve as scaffolding for the further growth of (2) fibrous skeleton. Based on transverse and longitudinal sections and histochemical staining techniques, I demonstrate herein that in extant corals (i.e., *Stephanocyathus*, *Flabellum*, *Desmophyllum*, “*Ceratotrochus*”, *Galaxea*, *Platygyra*), the entire septal skeleton is composed of superimposed layers of mineral and organic-enriched phases. These may be interrupted in some directions of growth but in other directions there is continuity between “centers of calcification” and “fibers”, making any distinction between these two structures unclear. As an alternative to the “two-step model”, a “layered model” of skeletal growth is proposed, that explains the differences between “centers of calcification” and “fibers” in terms of differential growth dynamics between these regions. Instead of the traditional but inadequate “trabecular” and “centers of calcification” concepts, a distinction between deposits of the Rapid Accretion Front (dRAF; which in particular cases can be organized into Centers of Rapid Accretion (CRA), and Thickening Deposits (TD) is proposed. In the dRAF region, mineral components, ca. 50 nm in diameter, seem to match the size range of nodular structures recently interpreted as nascent CaCO<sub>3</sub> crystals. Remarkable regularity of the mineral/organic phase alternations (microbanding) in the TD skeleton of zooxanthellate corals and lack of such regular microbanding in azooxanthellate coralla is a promising criterion for distinguishing these two ecological coral groups on a skeletal basis, and one that could be applicable to fossils.

Key words: Scleractinia, biomineralization, microstructures, nanostructures, “centers of calcification”, fibers.

Jarosław Stolarski [stolacy@twarda.pan.pl], Instytut Paleobiologii PAN, Twarda 51/55, 00-818 Warszawa, Poland.

## Introduction

For more than a century, microscopic features of the skeleton have been considered paramount in elucidating evolutionary relationships of Scleractinia and as basic classification criteria. A coherent and still widely used classification by Vaughan and Wells (1943), amended by Wells (1956), has most diagnoses of higher-level taxa based on microstructural characters of septa, e.g., the pattern of arrangement of “centers of calcification” from which aragonitic fibers radiate to form more complex units, traditionally called sclerodermites and/or trabeculae (see also Stolarski and Roniewicz 2001). In modern biological science this represents a rare instance of a classification proposed long ago by paleontologists, and thus based mostly on hard-parts, still being used by students of living taxa. Basic characters of the coral skeleton, reduced to the distribution pattern of septal “centers of calcification”, gained acceptance among taxonomists because implementation of anatomical characters of polyps failed (e.g., Duerden 1902; Matthai 1914), and many macro-morphological characters proved to be homeomorphic in nature. The microstructural approach to the coral skeleton has been found use-

ful by paleontologists seeking criteria to revise old generic and supra-generic catch-all taxa (e.g., revisions of “*Montlivaltia*” by Gill and Lafuste 1971, or traditional guyniids by Stolarski 2000), or to supplement databases of morphologic characters of coralla accessible from thin-sectioned rock samples (e.g., Roniewicz 1989).

In spite of the importance of minute-scale skeletal structures in coral phylogenetics, organismic control of their formation has thus far been poorly understood. Only recently, new analytical approaches have been proposed that ultimately may lead to the re-assessment of biological, and hence taxonomic, meaning of these structures. These include: (1) precise monitoring of various biochemical parameters at biomineralization sites with the aid of microelectrodes (De Beer et al. 2000; Al-Horani et al. 2003), (2) preparations of frozen-hydrated coral samples that allow high-resolution Field Emission Scanning Electron Microscope (FESEM), histological observations and x-ray microanalyses of the nearly intact tissue/skeleton interface (e.g., Clode and Marshall 2002, 2003a, b), (3) spectroscopic and histochemical staining techniques (Cuif et al. 1997; Cuif and Dauphin 1998; Cuif, Dauphin, and Gautret 1999), including advanced X-ray-Absorption Near Edge struc-

ture Spectroscopy (XANES) fluorescence (Cuif, Dauphin et al. 2003), which provide insights into composition and spatial distribution of intraskeletal organic components. Recent studies of the primary structure and expression of individual exoskeleton proteins and their possible role in calcification or interaction with other components of the organic matrix (Fukuda et al. 2003) herald still more novel approaches to a more integral understanding of scleractinian biocalcification.

However, explanation of organismic control upon the formation of minute-scale structures may be only as accurate as accurate are descriptions of these structures. The most up-to-date model of formation of minute-scale structures focuses on the role of organic components in the formation of structurally and biochemically distinct regions of "centers of calcification" and fibers (Cuif and Sorauf 2001). In recent literature, the illustrative basis depicting differences between "centers of calcification" and fibers and the ontogenetic development of these structures are, almost invariably, transverse sections of septa or close-ups of their distal edges (compare e.g., Cuif and Dauphin 1998). Interestingly, only at the beginning of the boom of modern microstructural studies in the 1970s, some effort was undertaken to register actual ontogenetic variation of microstructures in skeletal elements sectioned longitudinally (Wise et al. 1970; Wise 1972; and particularly Jell and Hill 1974; Jell 1974). Since that time, however, no attempts were made to develop a truly three-dimensional model of corallum growth that would make use of recent advances in understanding coral biomineralization based on differently oriented sections, particularly longitudinal ones. The objective of this paper is to fill this gap and, through the use of precisely oriented sections, trace ontogenetic changes in the distribution of mineral and organic components of the skeleton. This approach not only casts light on the development of minute structures in modern deep-water (azooxanthellate) and shallow-water (zooxanthellate) corals, but also allows the reinterpretation of formation of skeletal structures in some diagenetically unaltered and altered fossil corals, especially stylophyllids that traditionally were considered distinct from modern Scleractinia (compare Stolarski and Russo 2002). Another aim of this study is a critical review of traditional microstructural terminology used in scleractinian studies.

## Materials and methods

Material used in this study consists of extant (azooxanthellate and zooxanthellate) and fossil scleractinians. Most data were obtained from transverse and longitudinal sections of septa. Longitudinal sections were made perpendicularly to the septum, or were oriented radially, precisely in the mid-septal zone. Such longitudinal-radial orientation allows one to trace ontogenetic changes of structures formed in the region exhibiting the fastest growth rate and determining the shape of the skeleton. Traditionally, deposits formed in this region are referred to as "centers of calcification" or trabeculae; however,

these terms inadequately describe reality (see Discussion). Hence, new terminology referring to differences in growth dynamics is suggested herein (see also Glossary, p. 526). Distal-most regions of various skeletal elements (including lateral septal "ornamentation"), but especially of the septal growing edge, form the Rapid Accretion Front (RAF) which in some instances may split into Centers of Rapid Accretion (CRA). During ontogeny, deposits of the Rapid Accretion Front (dRAF) or Centers of Rapid Accretion (dCRA) are embedded within the skeleton that may gain a considerable thickness, being covered by Thickening Deposits (TD, which traditionally are called stereome if they are intracalicular, and tectura if they are extracalicular; details in Stolarski 1995). Because the RAF often follows an undulating or zigzag course, both in transverse and/or longitudinal planes, it is difficult to obtain large sections positioned precisely in the plane of the RAF. Among the specimens examined, the first satisfactory longitudinal-radial sections were obtained from the coralla of *Stephanocyathus paliferus* Cairns 1977; thus, skeletal analysis of this coral is the starting point of this study. The use of the skeleton of *Stephanocyathus* Seguenza, 1864 has the added advantage in that extant and fossil representatives of this genus have earlier been the subject of microstructural studies (Sorauf and Podoff 1977; Stolarski 1990) and hence, allow for comparison of new observations with former descriptions.

In this study, the corallum of *S. paliferus* was studied using conventional transmitted light microscope (TLM), molecular fluorescence microscope (MFM), scanning electron microscope (SEM), and atomic force microscope (AFM). The skeleton was fixed with araldite and polished with aluminium oxide (Buehler TOPOL 3 final polishing suspension with particle size 0.25 µm). After polishing, the sections were rinsed in distilled water and washed in an ultrasonic cleaner for 10 seconds. Polished sections prepared in this way were examined using the AFM microscope. For MFM observations, sections were examined unstained (autofluorescence) or stained in a 0.45 µm filtered, 1% acridine orange (Sigma-Aldrich prod. #A-6014) aqueous solution for 5 minutes. Acridine orange is a cationic dye whose chromatic response is affected by the gross secondary structure of the organic substrate, concentrations of adsorbed molecules, pH, temperature and ionic strength (see also Gautret et al. 2000). Stained samples were briefly rinsed in distilled water, air dried and photographed with a Nikon Eclipse E-800 light microscope fitted with epi-fluorescence attachment and Nikon DXM 1200 digital camera. Micrographs were taken using a 494 nm excitation filter and 520 nm emission filter. For SEM observations, sections were exposed for 30–60 seconds to a solution of 0.1% formic acid, then rinsed in distilled water and air-dried. Formic acid is known to dissolve not only mineral but also organic components (such as proteins) that are not stabilized by covalent bonds (Waite and Anderson 1980).

Transverse and longitudinal sections in the RAF plane were obtained also from: (1) azooxanthellates: *Flabellum chunii* Marenzeller, 1904, *Desmophyllum dianthus* (Esper, 1794), "*Ceratotrochus*" *magnaghii* Cecchini, 1914 (and not

figured: *Caryophyllia cyathus* (Ellis and Solander, 1786), *Deltocyathus eccentricus* Cairns, 1979, *Fungiacyathus pusillus pacificus* Cairns, 1995, *Trochocyathus rawsonii* Pourtalès, 1874, *Anthemiphyllia dentata* (Alcock, 1902), *Javania insignis* Duncan, 1876, *Stephanocyathus* (*Acinocyathus*) *spiniger* (Marenzeller, 1888), *Paracyathus pulchellus* (Philippi, 1842), and *Vaughanella concinna* Gravier, 1915), and (2) zooxanthellates *Galaxea fascicularis* (Linnaeus, 1767), *Platygyra daedalea* (Ellis and Solander, 1786), and not figured *Favia* sp. and *Hydnophora* sp. Polished sections of these coral samples were examined using TLM, MFM, and SEM microscope techniques.

Elemental (C, S, Sr, Mg) X-ray mapping of some coralla (e.g., here illustrated carbon mapping of *Flabellum chunii* Marenzeller, 1904 and Sr, Mg mapping of *Pachysolenia cylindrica* Cuif, 1975) were acquired on a Cameca SX-100 electron microprobe using wavelength-dispersive techniques (WDS) at the Inter-Institute Analytical Complex for Minerals and Synthetic Substances, Electron Microprobe Laboratory (Department of Geology, Warsaw University). The following parameters were used during stage scan: 15 kV (accelerating voltage), 20 nA (beam current), 60 msec (pixel time), and ca. 1 mm spacing (515×515 pixel resolution). Back-scattered electron (BSE) images that enhance atomic number contrast have also been collected. Specimens were coated with platinum of ca. 2 nm thickness.

*Institutional abbreviations.*—IPUM, Institute of Paleontology, University of Modena, Italy; NMNH, National Museum of Natural History, Smithsonian Institution, Washington, D.C.; ZPAL, Institute of Paleobiology, Polish Academy of Sciences, Warsaw.

## Extant azooxanthellate *Stephanocyathus paliferus* Cairns, 1977

*Septal morphology.*—Septa have a smooth, non-denticulated distal margin typical of traditional caryophyllinans (Fig. 1A–C)<sup>1</sup>. SEM close-ups of the septal margin show slightly irregular, rounded “patches” (ca. 5–20 µm in diameter) whose surface has a grainy texture, which results in the exposure of angular or somewhat rounded “microcrystalline” components, 300–500 nm in diameter (Fig. 1E). These “patches” cover the entire length of the distal septal margin, which is rounded and only 50–100 µm wide. In places, the straight course of the distal margin has a zigzag deviation to sites with granular or longitudinal ridge-like structures (“ornamentation”) appearing on septal flanks (Fig. 1D). The septal surface between granulae is smooth.

*Transverse sections.*—Two zones of different light-transparency properties and colors are distinguishable in transverse sections made approximately throughout half the length of S1 and viewed in TLM (Fig. 2C): (1) a dRAF zone (mid-septal zone), with darker, slightly opaque brownish coloration (“dark line”), and (2) a TD zone of transparent, nearly colorless fibers, that borders the dRAF zone. The dRAF zone has a slightly wavy course and is ca. 50 µm in width; it is not homogenous but is composed of rounded spots (ca. 20 µm in diameter) with a higher concentration of dark brown components that are fairly regularly distributed. The skeleton adjacent to the dRAF zone is composed of bundles of fibers (TD), quasi-perpendicularly orientated to the dRAF plane. In MFM, skeleton stained with acridine orange dye exhibits a twofold chromatic response (Fig. 2D). Patches exhibiting bright green fluorescence perfectly match those in TLM having brown coloration within the dRAF zone. Chromatic response of TD is much less prominent, and green-orange fluorescence is localized at borders between fibrous layers and also at borders between individual bundles of fibers. In polished, etched sections (SEM), dRAF exhibits a negative relief, whereas TD generally shows positive etching relief, except for the borders between layers of fibers (especially borders parallel to septal faces; Fig. 3A). On the bottom of dRAF etched hollows some crystalline structures can be discerned (Fig. 3B).

*Longitudinal-radial sections.*—Fig. 2A shows an S1 in TLM cut precisely in the mid-septal plane. Due to the slightly undulating course of RAF, dRAF are not visible on the entire surface of this thin-section. In fact, only some brownish spots that mark the position of sectioned dRAF (Fig. 2A, B) are those that are truly exposed; some others are located slightly beneath the surface of the section and visible only using transmitted light (and not SEM, for example). In spots where dRAF are easily visible (Fig. 2B–E) they form “strands” ca. 20–30 µm in width more or less parallel to each other; however, they are arranged fanwise in the plane of the entire section (Fig. 2A). Each “strand” is composed of regular alternations of thicker, brownish, and slightly opaque layers (ca. 5–6 µm width) that are intercalated with thin, rather colorless and more transparent ones (ca. 1.5–2 µm width). Layers within each “strand” have domed shapes, and fade approaching the border of the “strand” (Fig. 2E, yellow arrow), or may continue between “strands” (Fig. 2E, pink arrow). Only those layers that are brownish in TLM exhibit strong, bright green fluorescence in MFM, whereas thin and transparent layers do not show a chromatic reaction (Fig. 2F). Some corresponding “strands” (compare Fig. 2E and Fig. 2F) do not exhibit in MFM strong chromatic reaction, most likely because some “strands” are actually located inside the thin-section as mentioned above, hence, were not exposed to the

<sup>1</sup> Stolarski (2000) showed that the seemingly smooth distal edge of the septa in some caryophyllinans (i.e., traditional guyniids), as seen at lower magnification, may actually consist of tiny denticulations (*Stenocyathus*, *Truncatoguynia*) or indeed, be nearly completely smooth at higher magnification (*Guynia*). In this respect, the distal septal margin of *S. paliferus* is intermediate between that of *Guynia* and *Stenocyathus*, and resembles especially that of *Lophelia pertusa* (Linnaeus, 1758), described as “built of densely packed accumulation of centers of calcification” (Cuif and Dauphin 1998: 263, fig. 3.7).

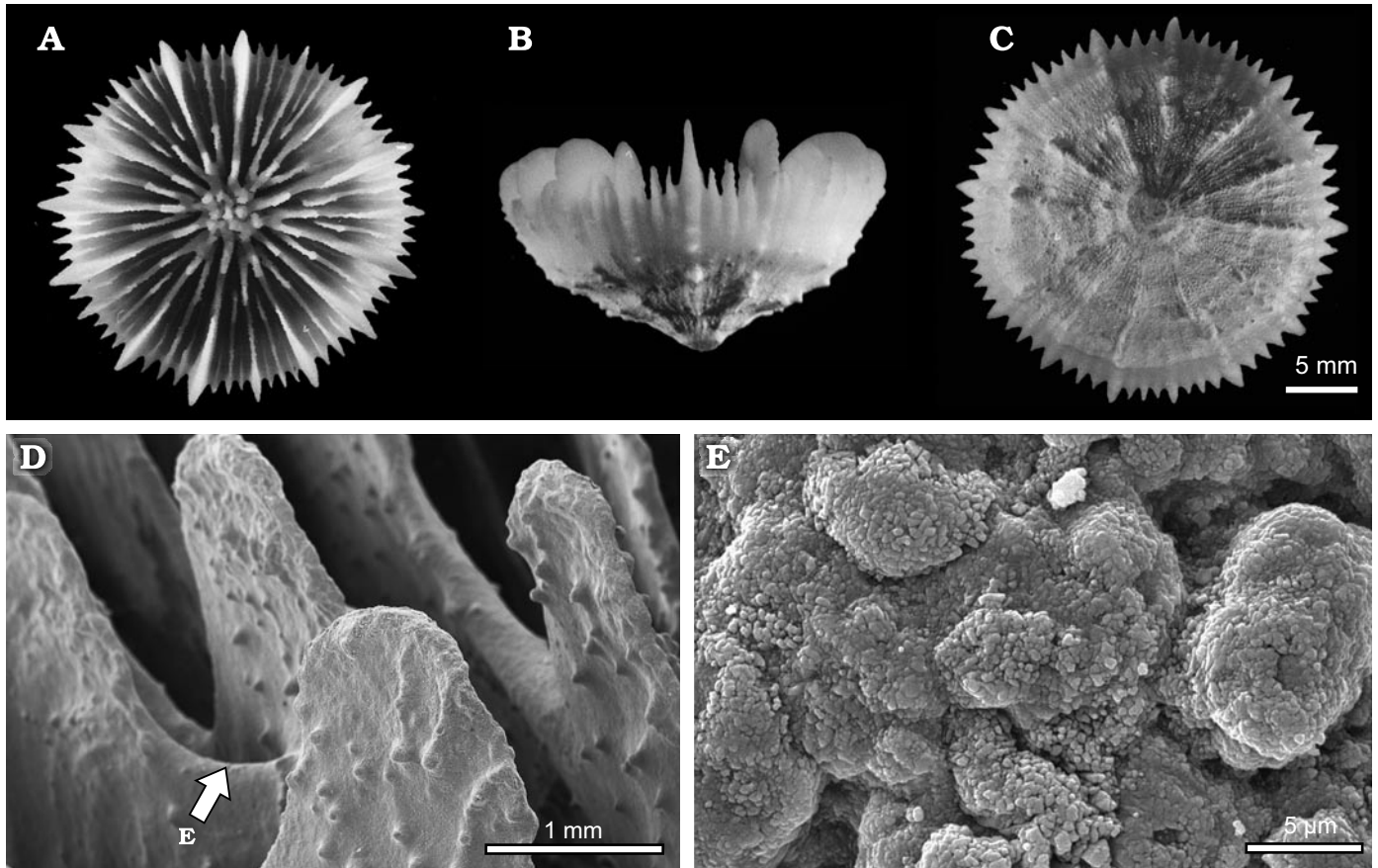


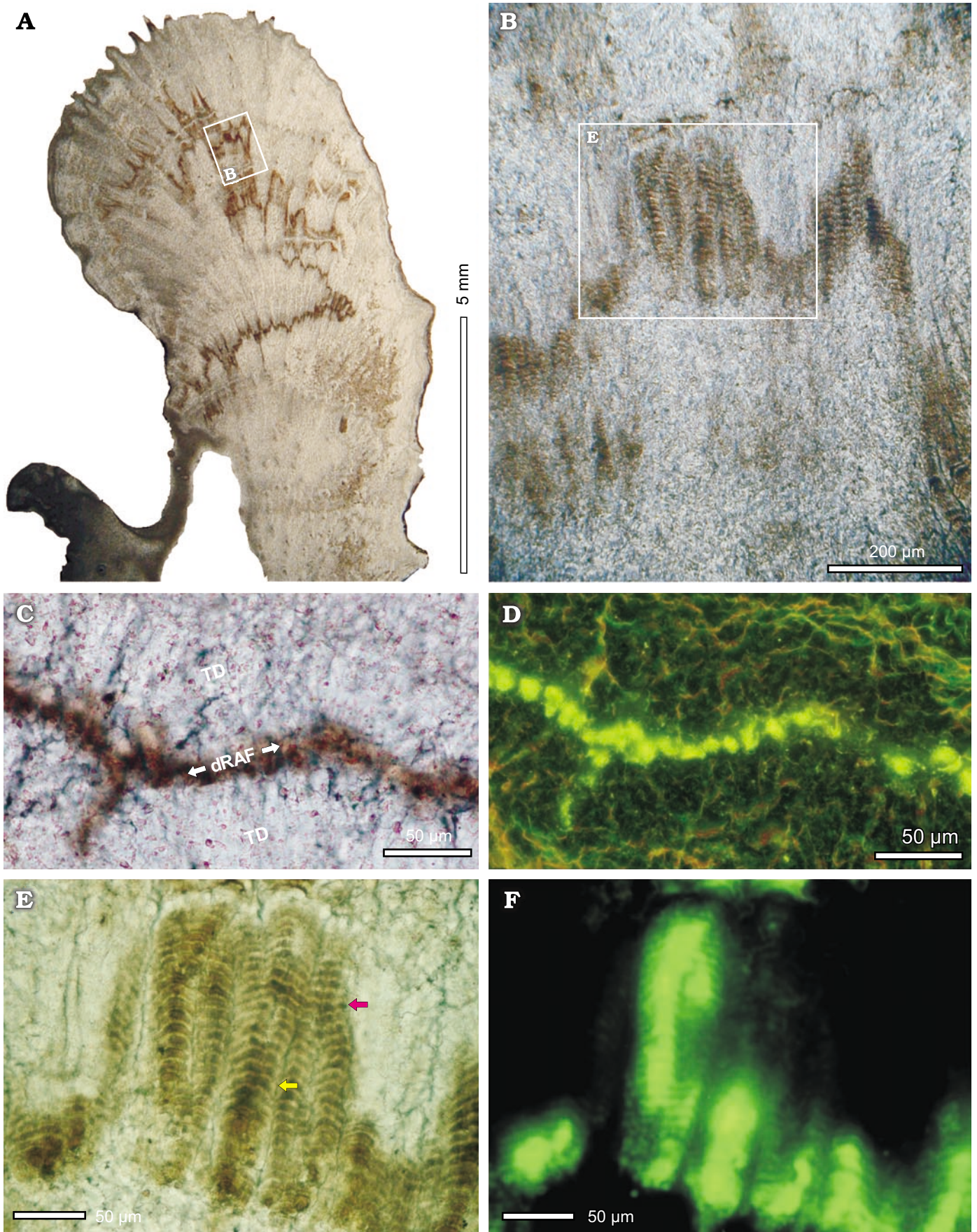
Fig. 1. *Stephanocyathus paliferus* Cairns, 1977. ZPAL H.23/1 (originally NMNH 46443 lot). Recent, south of Bonaire, 11°18.8'N, 68°22'W, 384–607 m. Pills sta. P-753. July 26, 1968. A–C. Distal (A), lateral (B), and proximal (C) views of corallum. D, E. SEM of septa and paliform lobes. D. Arrow indicates portion of septum enlarged on E. E. “Patches of microcrystals” (fasciculi of Wise 1972) at the growing septal edge here called the Rapid Accretion Front (RAF).

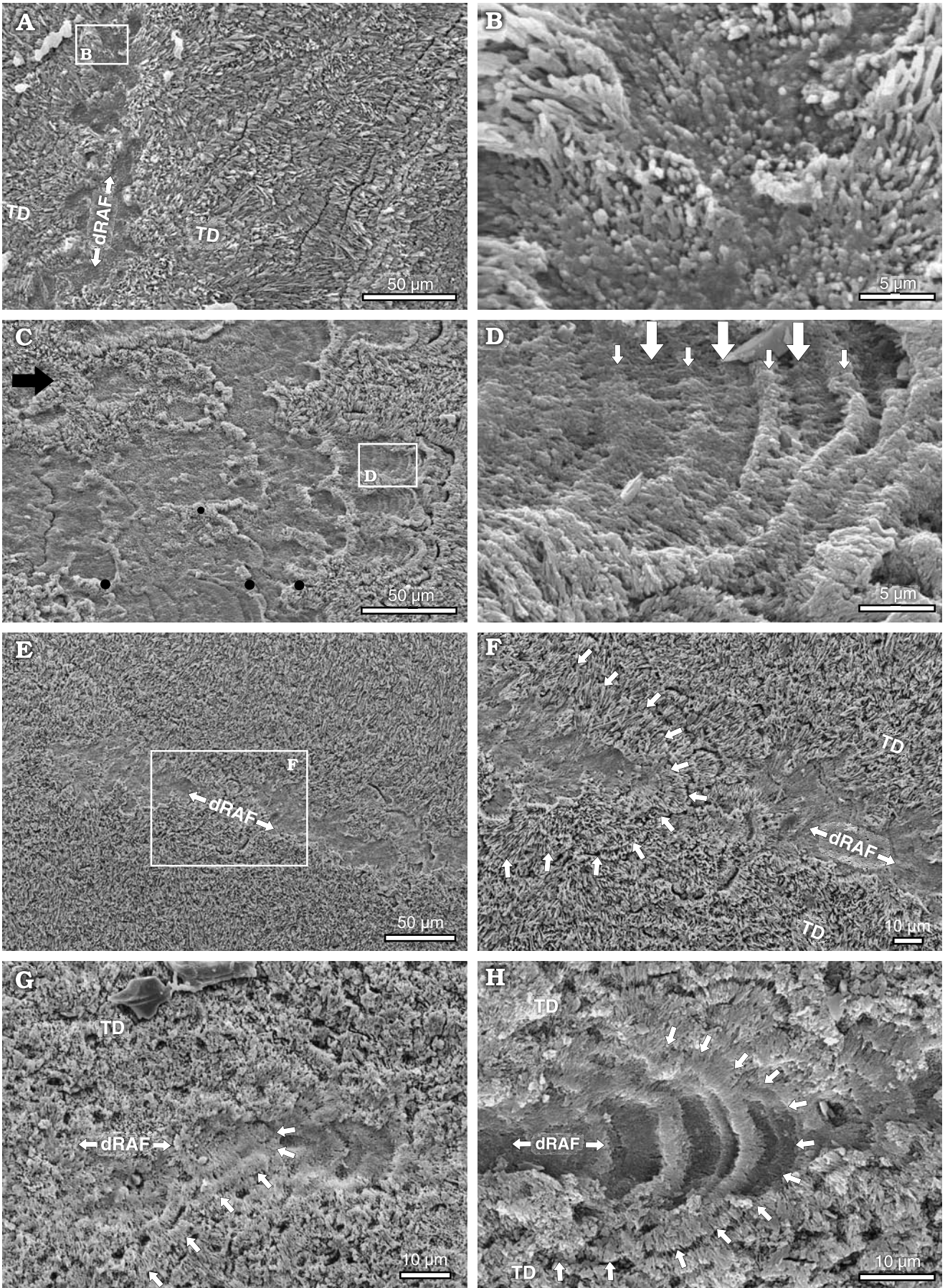
acidine orange dye. Scanning electron micrographs of polished and etched sections correspond to those viewed in TLM: ca. 20–30 µm wide “strands” of generally negative etching relief are composed of regular alternations of domed hollows (ca. 5–6 µm width), separated by small and narrow ridges (ca. 1.5–2 µm width), Fig. 3C, D. Layers within each “strand” fade approaching the border of the “strand” or continue between neighboring “strands” (Fig. 3C). The narrow ridges are composed of fibers perpendicular to their course; similar but longer fibers are seen in the bottom of wider etching hollows. At higher magnifications, fibers that form ridges or are visible on the bottom of hollows exhibit a lumpy texture. Polished (but not etched) sections prepared for use in AFM, show very small and shallow grooves, difficult to discern under low magnification of a dissection scope. AFM images of these hollows reveal aggregations of grains that are ca. 50 nm in diameter (Fig. 4A–E). Their size most likely matches that of lumps on fibers viewed in SEM; however,

because of better resolution the size of these particles is based on AFM observations. The skeleton bordering shallow grooves also shows, in some places, nanogranular texture, however, only in grooves individual grains are well exposed.

*Section perpendicular to the septal plane.*—In this section, only one, relatively narrow region of dRAF occurs. Fig. 3E, F shows a polished, lightly etched section with the dRAF region having negative relief, which is bordered with TD that have positive etching relief, except for the borders between layers of fibers. There is an overall continuity of layers of fibers between dRAF and TD; most fiber layers visible in the center of dRAF are still traceable within the TD. Only in some places individual layers visible in dRAF may disappear towards the TD. The basic difference between these two regions is a distinct negative etching relief of broader zones in dRAF, and only very narrow zones of negative relief at borders between fiber layers in TD.

Fig. 2. *Stephanocyathus paliferus* Cairns, 1977. ZPAL H.23/1. Locality data as in Fig. 1. A, B. TLM micrographs of longitudinal polished sections in RAF plane. C, D. Transverse polished section of septum in TLM (C) and MFM (D). Organic components of dRAF (brownish in C) stained with acridine orange show bright-green fluorescence (D). Chromatic response of TD is much less prominent. E, F. TLM (E) and MFM (F) micrographs of enlarged part of longitudinally sectioned septum shown in B. Organic and mineral phases of dRAF regularly alternate; only organic components exposed and stained with acridine orange fluoresce with bright-green light. →





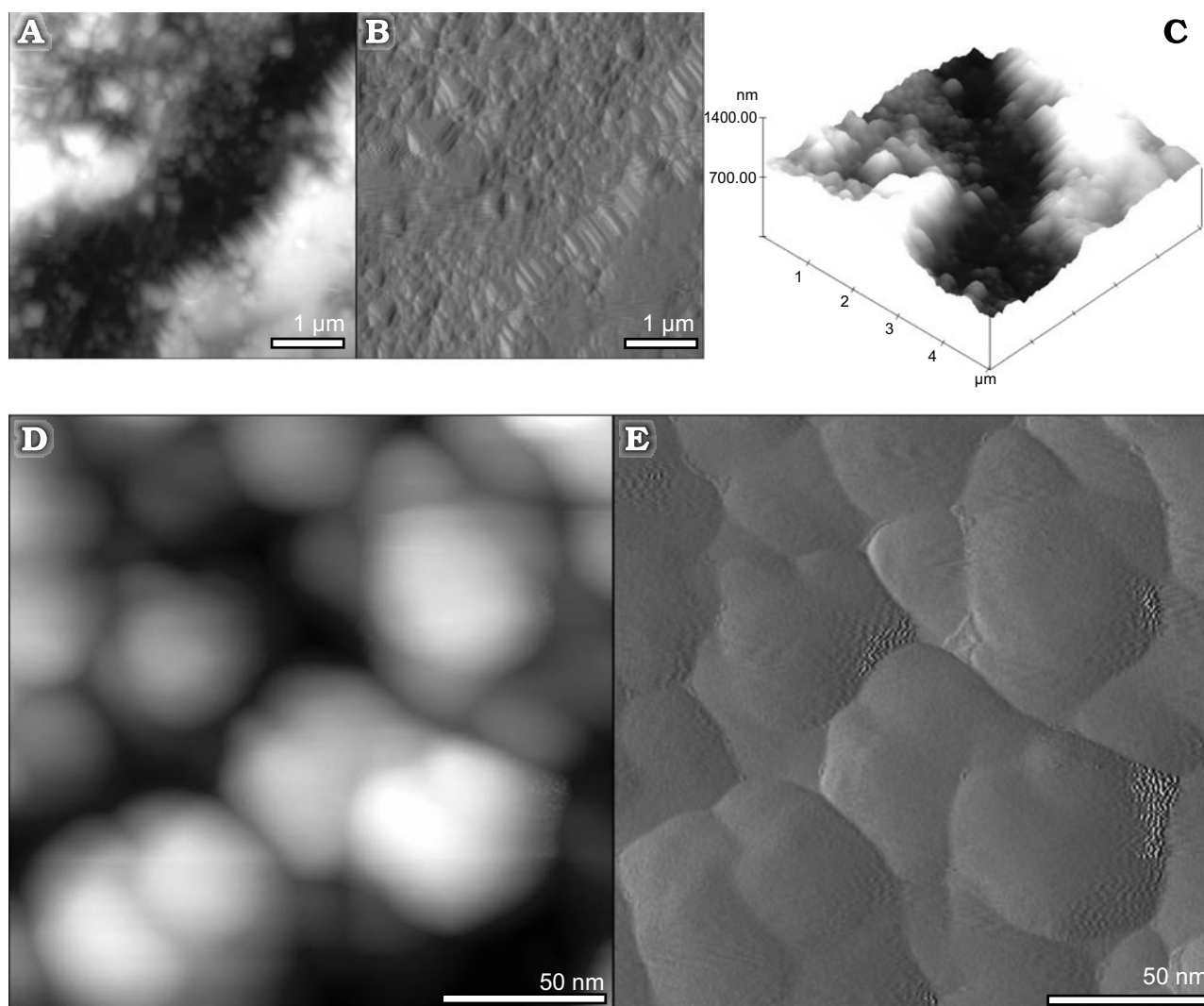


Fig. 4. *Stephanocyathus paliferus* Cairns 1977. ZPAL H.23/1. Locality data as in Fig. 1. **A–C.** AFM (contact mode): height—2D projection (**A**), phase (**B**), and height—3D projection (**C**) images of 5 μm polished (not etched) septum sectioned in RAF plane; AFM tip was placed in dRAF “strand” region as seen in etched sections (Fig. 3C). **D, E.** AFM (tapping mode) height—2D projection (**D**) and phase (**E**) images of spherical bodies seen on the bottom of dRAF “strand”.

## Other extant azooxanthellate scleractinians

### *Flabellum chunii* Marenzeller, 1904

**Septal morphology.**—*F. chunii* (and some other representatives of traditional Flabellidae) have a scale-like texture on the septal flanks (Fig. 5A<sub>1</sub>, A<sub>2</sub>). Scale-like units here are composed of bundles of fibers arranged quasi-parallel to

septal faces (in *Stephanocyathus* bundles of fibers are arranged quasi-perpendicularly to the septal faces resulting in their smooth surface). Scale-like structures are developed also on the inner side of the wall, and on the axial junction of the septa. Scale-like units continue on distal, growing edges of skeletal elements where they form small tubercles.

**Transverse sections.**—SEM micrograph of polished and etched sections made approximately in half of the length of S1 (Fig. 5D<sub>1</sub>, D<sub>2</sub>), shows two zones of different etching relief: (1) dRAF zone (mid-septal zone) composed of series of

← Fig. 3. *Stephanocyathus paliferus* Cairns 1977. ZPAL H.23/1. Locality data as in Fig. 1. SEM of polished and etched septal sections. **A, B.** Septum transversely sectioned with two distinct zones: dRAF and layers of TD. dRAF, as viewed from this perspective, may be considered to consist of a homogeneous zone of “microcrystals” (only crystal tips visible; see enlargement in B) and this interpretation traditionally prevailed. **C, D.** Septum longitudinally sectioned in RAF plane (growth direction of septum indicated by black arrow in C). **C.** Dissolved/etched components of dRAF form a pattern of longitudinal (horizontal in photo) “strands”, occasionally separated by small ridges (asterisk); wrinkles of adjacent “strands” form in places pronounced “rollers” (black dots). **D.** Enlarged “strand” with alternations of wider, domed cavities (larger arrows) and narrow ridges (small arrows) that match organic and, respectively, mineral phase alternations in Fig. 2E, F. **E–H.** Sections perpendicular to septal blade. Fibrous layers continue between dRAF and TD deposits (arrows in F–H).

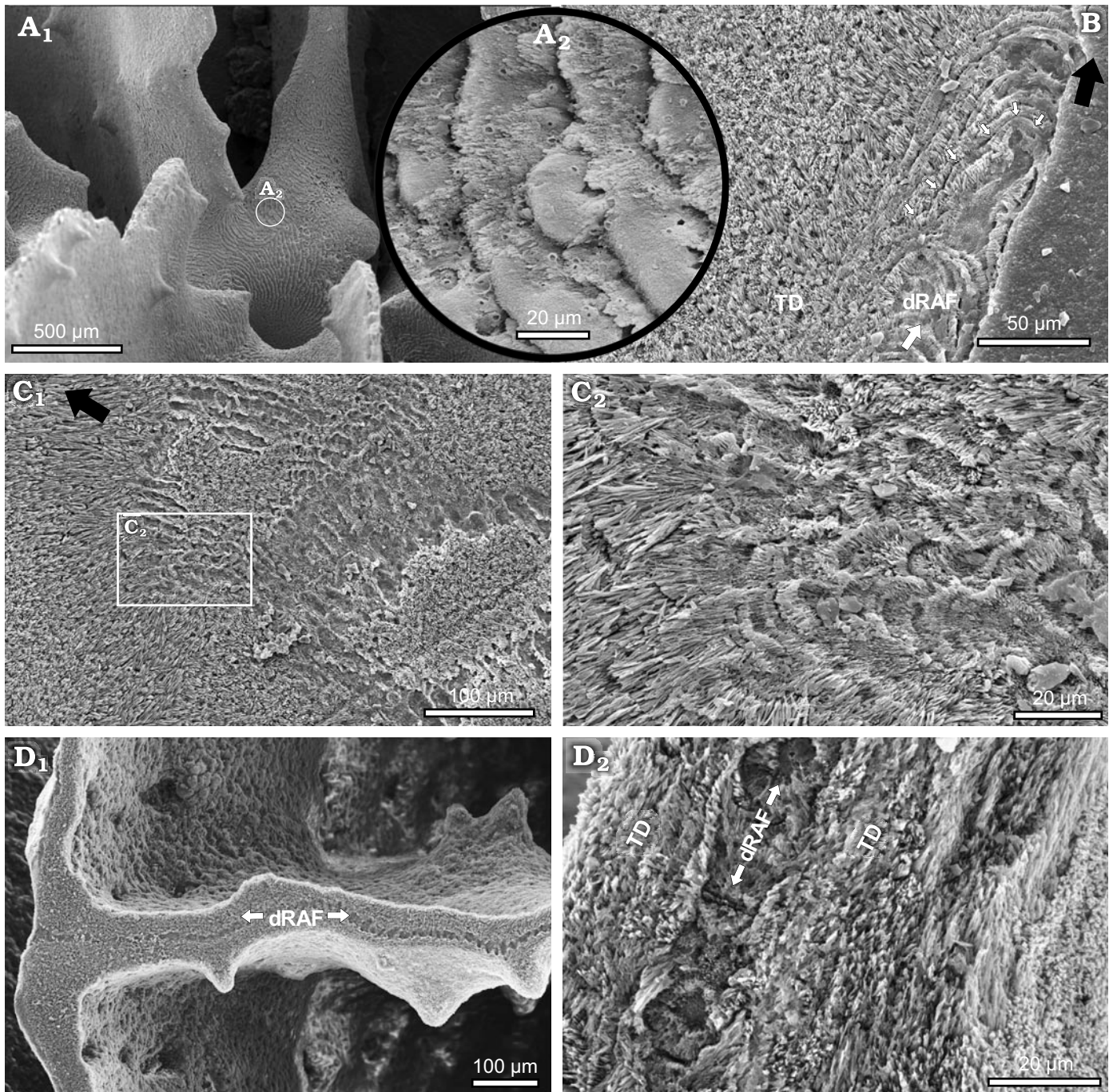


Fig. 5. *Flabellum chunii* Marenzeller, 1904. Recent, Great Meteor Seamount, SEAMOUNT2 (1993), DW 152 (January 11, 1993), 30°02.00'N, 28°22.10'W, 470 m. **A.** Septa and inner side of wall ( $A_1$ ) thickened by fibers arranged in scale-like units ( $A_2$ , enlargement); ZPAL H.23/2/1. **B.** Marginothecal wall sectioned longitudinally (large white arrow); layers of successive growth increments (dRAF) continue in wall "stereome", i.e., TD (small white arrows); ZPAL H.23/2/2. **C.** Septum longitudinally sectioned in RAF plane. Dissolved or etched components of RAF form narrow "strands" ( $C_2$  enlargement); ZPAL H.23/2/3. **D.** Transverse polished and etched section of septum; dRAF zone composed of neighboring dCRA ( $D_1$ ) is from both sides covered with layers of TD fibers ( $D_2$ ) which direction conform to that of scale-like units (i.e., semi-parallel to RAF); ZPAL H.23/2/4. All SEM; growth direction within skeletal element indicated by black arrow in B.

neighboring pits (dCRA), and (2) TD zone composed of layers of fibers orientated quasi-parallel to the septal surface.

The dCRA show twofold structure: inner, deeper hollow is surrounded with circle of short fibers (Fig. 5D<sub>2</sub>). The dRAF zone continue between septa and wall (marginotheca, see Stolarski 1995).

*Longitudinal-radial sections.*—Longitudinal sections in the RAF plane show narrow "strands" (ca. 15 μm in width) that are arranged fanwise in the plane of the section (Fig. 6D). Due to the undulating course of RAF in radial and longitudinal directions, dRAF are visible only in some surfaces of the thin-section. In TLM, each "strand" is composed of regular

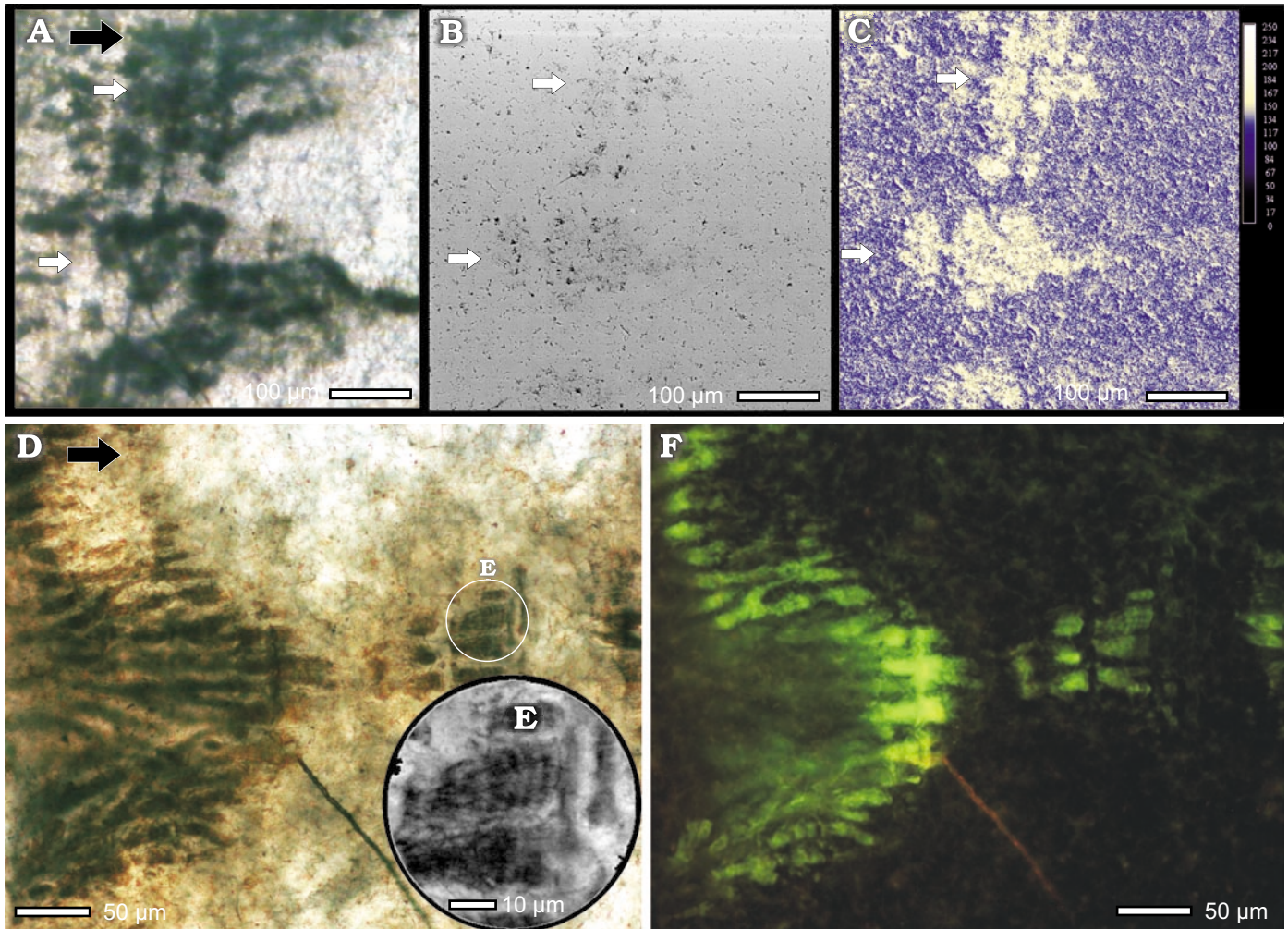


Fig. 6. *Flabellum chunii* Marenzeller, 1904. ZPAL H.23/2/4. Locality data as in Fig. 5. A–C. Complementary regions of longitudinally sectioned and polished septum (RAF plane): TLM (A), Back-Scattered Electron mode (BSE) (B), and pseudocolor carbon mapping images acquired on the electron microprobe by wavelength-dispersive techniques (C); black/dark blue equals lower concentration (<150 counts per second) whereas yellow-white equals higher concentrations (>150 c/s). Brownish structures exposed at section surface (A), appear darker in BSE mode (B) as it enhances atomic number contrast; elements with lower atomic numbers appear darker, those with higher atomic numbers appear lighter. BSE darker regions (arrows) match exactly to carbon-enriched regions in WDS x-ray mapping image (C, arrows). D–F. TLM (D, E) and MFM (F) micrographs of longitudinally sectioned septum. Organic and mineral phase of dRAF regularly alternate (grayscale enlargement in E); brownish organic components (D) exposed and stained with acridine orange dye, fluoresce (F) with bright-green light. Growth direction within septum indicated by black arrow.

alternations (Fig. 6E) of thicker, brownish, and slightly opaque layers (ca. 1–3  $\mu\text{m}$  width) that are intercalated with thin, rather colorless and more transparent ones (ca. 0.8–1  $\mu\text{m}$  width). Layers within each “strand” have domed shapes, and fade approaching the border of the “strand”. Layers that are brownish in TLM exhibit strong, bright green fluorescence in MFM; thin and transparent layers do not show a chromatic reaction (Fig. 6F). Polished and etched sections viewed in SEM (Fig. 5C<sub>1</sub>, C<sub>2</sub>) show ca. 15  $\mu\text{m}$  wide “strands” of generally negative etching relief that are composed of regular alternations of domed hollows (ca. 2–3  $\mu\text{m}$  width), separated by small and narrow ridges (ca. 1.5–2  $\mu\text{m}$  width).

Elemental (C, S, Sr, Mg) X-ray mapping of polished sections using wavelength-dispersive techniques (WDS) showed an overall homogenous distribution of S, Sr and Mg

(the latter is a trace element). However, “strands” as viewed in TLM (Fig. 6A), or darker regions as viewed in BSE mode (Fig. 6B), are enriched in carbon (Fig. 6C).

*Section perpendicular to the wall.*—Polished and etched sections perpendicular to the marginothecal wall (Fig. 5B) show overall continuity of layers of fibers between dRAF and TD. The main difference between these regions is negative etching relief of broader zones in dRAF region and only narrow zones of negative relief between fiber layers in TD; pattern of layers continuing between dRAF and TD zones is very similar to that observed in *S. paliferus* in section perpendicular to the septum, however, in *Flabellum* TD are formed primarily on the inner wall side (layers that continue on outer side of the wall, named tectura by Stolarski (1995), are narrow and fade downwards).

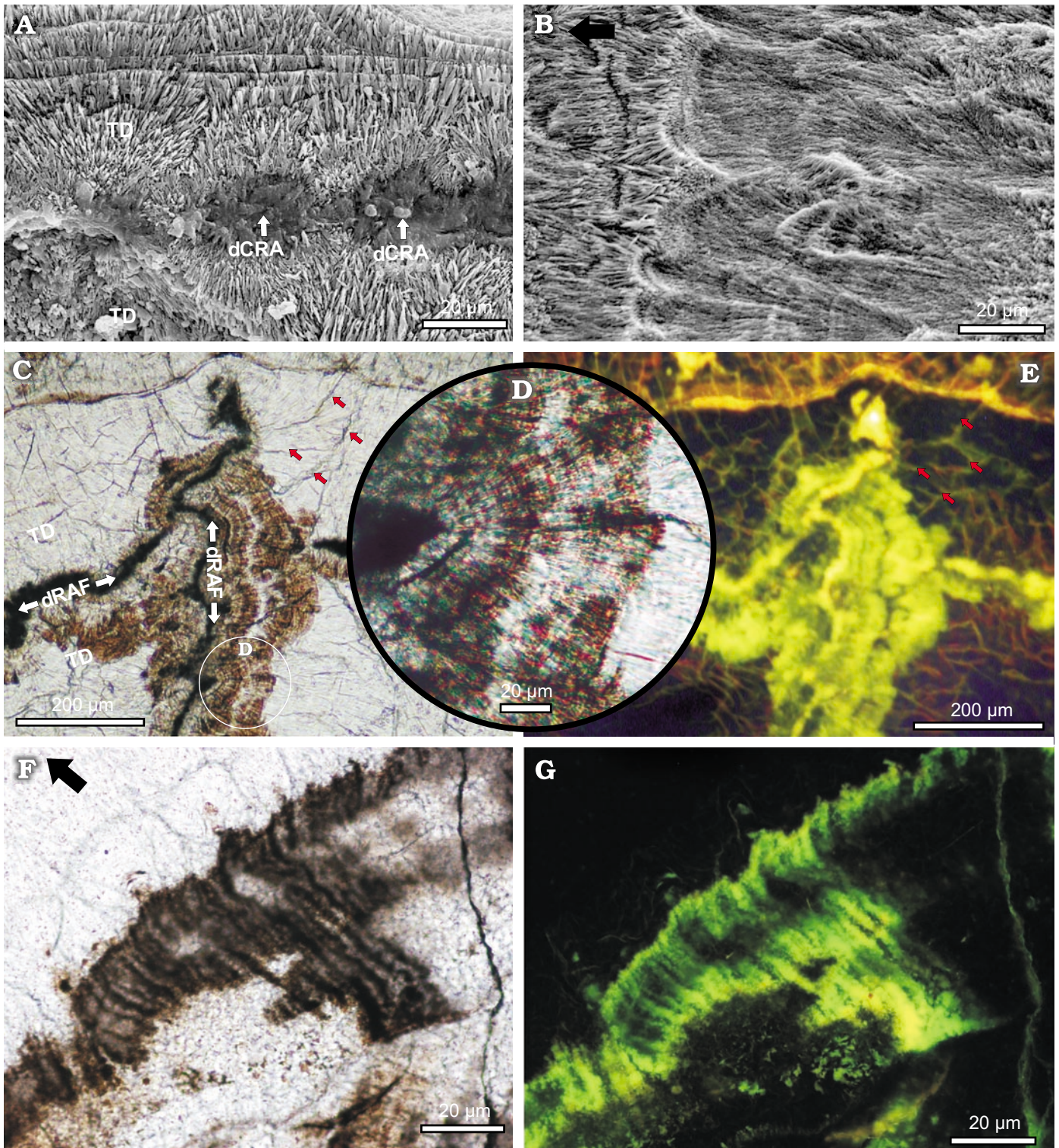


Fig. 7. *Desmophyllum dianthus* (Esper, 1794). ZPAL H.23/3. Recent, southern Indian Ocean (NE St. Paul Island), MD50 cruise, Stat. 32/CP 145, 38°40.66'S, 77°35.47'E, 825–1020 m. **A, B.** Polished and etched septum sectioned transversely (**A**) and longitudinally in RAF plane (**B**). dRAF form chain of dCRA (“centers of calcification”) (**A**), which sectioned longitudinally exhibit alternating etching relief (**B**). dCRA (**A**) are composed of apparently non-crystalline, “blurry” material. **C–E.** Transverse polished section of septum in TLM (**C, D**) and MFM (**E**) micrographs. In TLM (**C, D**) organic components differentiate into dark-brown zone of wall and septal dRAF and light-brown, banded zone enclosing dRAF; in MFM (**E**) they exhibit lighter, green-yellow, and darker, greenish fluorescence, respectively. Contact zone between bundles of fibers (also with apparent fractures) contain organic matter that forms a fluorescent network (**E**); examples highlighted with red arrows. **F, G.** Septum longitudinally sectioned in RAF plane in TLM (**F**) and MFM (**G**). Minute growth increments (less than 5  $\mu\text{m}$ ) appear as “denticulations” on fluorescent bars (**G**). Growth direction within septum indicated by black arrow.

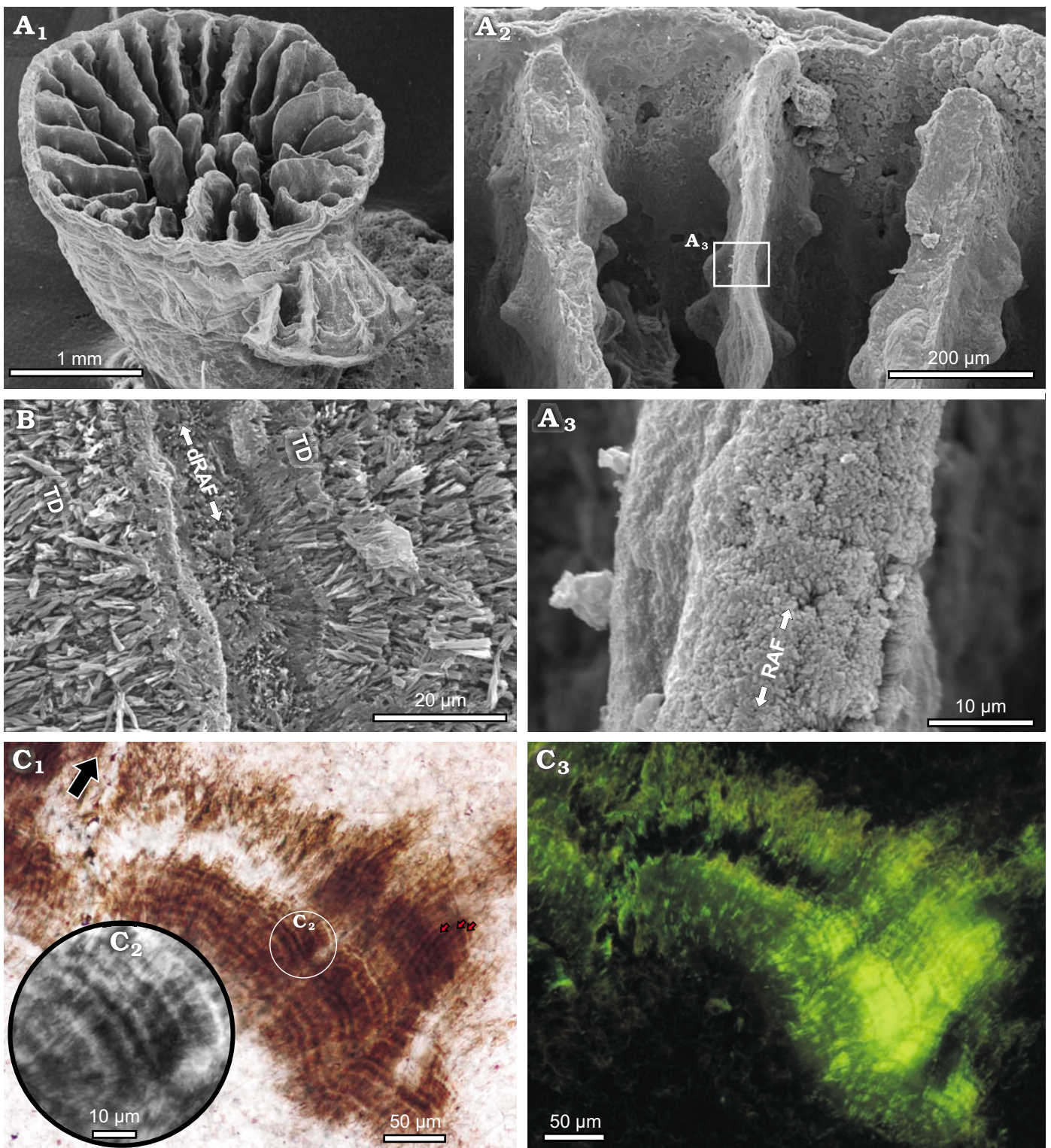


Fig. 8. “*Ceratotrochus*” *magnaghii* Cecchini, 1914. **A.** ZPAL H.23/4 in oblique view ( $A_1$ ); distal septal edge enlarged in  $A_2$ .  $A_3$ , “Patches of microcrystals” at growing septal edge (RAF). **B.** ZPAL H.23/5. Polished and etched septum sectioned transversely with dRAF that appear to be composed of homogenous “microcrystalline” material, SEM micrograph. **C.** TLM ( $C_1$ ,  $C_2$ ) and MFM ( $C_3$ ) micrographs of longitudinally sectioned septum ZPAL H.23/6 in RAF plane. Organic and mineral phases regularly alternate (grayscale enlargement in  $C_2$ ); brownish organic dRAF components ( $C_1$ ) stained with acridine orange, fluoresce ( $C_2$ ) with bright-green light. Seemingly homogenous dRAF in transverse section (**B**), sectioned longitudinally is composed of elongated units spaced ca. 5–7  $\mu\text{m}$  (red arrows in  $C_1$ ). Growth direction of septum indicates black arrow. **A.** Recent, deep-water specimen, SEAMOUNT 2 cruise, Stat. DW 279, 33°55.60'N, 28°23.70'W, 805 m. **B, C.** Recent, shallow-water specimen from Mediterranean (Marseille, Riou-Grand Conglu submarine cave), 50 m.

*Desmophyllum dianthus* (Esper, 1794)

**Morphology.**—The septal microarchitecture of *D. dianthus* is similar to that of *S. paliferus*. The distal septal margin is smooth in “macroscale” however, as viewed in SEM close-ups, its surface is composed of irregularly distributed rounded “patches”. They cover the entire length of the septal margin which is ca. 50 µm wide. The straight course of the distal margin may deviate in zigzag fashion towards granules on the septal flanks, however these are generally rare in the adult stage of corallum.

**Transverse sections.**—In TLM, three zones of different light-transparency properties and colors are distinguishable in transverse section of the S1 (made in half of its length) and part of the trabeculothecal wall (Fig. 7C): (1) dRAF zone ca. 15–20 µm wide, with a slightly wavy course and dark brown coloration (“dark line”), (2) zone (ca. 100 µm wide) of fibers with brownish zonal coloration (however, lighter than in dRAF zone), and (3) zone of transparent and nearly colorless fibers that form the main mass of the skeleton. The last two fibrous zones differ only in coloration, but show the same orientation of fibers or even their continuation. Generally, fibers are perpendicular to the dRAF zone, as in TD region in other corals discussed here (Fig. 7C, D). Fractures and/or very distinct natural borders occur between some bundles of fibers (Fig. 7C, red arrows). In MFM, skeleton stained with acridine orange dye exhibits a threefold chromatic response (Fig. 7E): (1) bright green fluorescence of narrow dRAF zone, (2) slightly weaker than of the former zone and green-yellow fluorescence of zone with brownish fibers as seen in TLM, and (3) near orange fluorescence of fractures or natural borders between fiber bundles in zone of transparent and colorless fibers as seen in TLM (Fig. 7E, red arrows). In SEM (Fig. 7A), polished and etched sections show distinct negative relief of the dRAF zone (ca. 15–20 µm wide, often differentiated into dCRA), whereas fibrous zones show generally positive etching relief, except for the borders between layers of fibers. Fibers enclosing the dRAF zone form a distinct region ca. 20 µm wide, beyond which layers of fibers show much smaller (ca. 5 µm wide) growth increments.

**Longitudinal-radial sections.**—In TLM, sections made in RAF plane show narrow dark brown “strands” (ca. 10–15 µm wide) arranged fanwise in the plane of the section (Fig. 7F). Similarly, as in the longitudinal sections of the above described corals, the undulating course of the RAF in radial and longitudinal directions makes the dRAF visible only in some surfaces. In higher magnification, extremely fine (ca. 2 µm long), regular constrictions of “strands” are visible; however, perhaps because of the standard (not ultra-thin) thickness of the section, it cannot be clearly stated whether constrictions correspond to regular alternations of transparent colorless and more opaque brownish layers as in other corals. Also inconclusive in this respect were observations in MFM, however, similarly as in other corals investigated, only the areas of brownish “strands” exhibited bright green-yellow fluorescence (Fig. 7G). In SEM, polished and etched sections show

ca. 10–15 µm wide “strands” (Fig. 7B) that generally have a negative etched relief; occasionally individual “strands” are not clearly delimited from each other, but rather form broader areas of negative relief. In the longitudinal direction “strands” show the alternation of zones more and less susceptible to etching. In places this alternation is very dense and regular (every 2 µm), and occasionally are less regular with wider zones more susceptible to etching (ca. 10 µm and more).

*“Ceratotrochus” magnaghii* Cecchini, 1914

**Morphology.**—Overall, septa of “*C.*” *magnaghii* have smooth distal margins as in *S. paliferus* and *D. dianthus*. However, in contrast to the previous two species, they remain nearly completely smooth, even in much higher magnification (Fig. 8A<sub>1</sub>, A<sub>2</sub>). SEM enlargement of distal septal margins shows their smooth surface, which is not differentiated into “patches” or tubercles. Similarly to e.g., *S. paliferus*, the structure of the septal margin regular “grains” ca. 500nm in diameter can be distinguished (Fig. 8A<sub>3</sub>). The generally straight course of the ca. 15 µm wide distal septal margin may show a gently zigzagging deviation towards granules on the septal flanks. Except for granulations, the septal surface is smooth.

**Transverse sections.**—Two zones of different etching relief can be distinguished in SEM view of sections made approximately in half of S1 (Fig. 8B): (1) a homogenous dRAF zone ca. 15 µm wide that has negative etching relief, and (2) TD zone of overall positive relief, except for the borders between bundles of fibers that are distributed more or less regularly every 7–10 µm.

**Longitudinal-radial sections.**—In contrast to a seemingly homogenous structure of dRAF zone as seen in SEM, longitudinal sections in the RAF plane reveal very narrow strands, ca. 5 µm wide and approximately parallel to each other but arranged fanwise in the plane of the entire section (Fig. 8C<sub>1</sub>, red arrows). These longitudinal “strands” have a layered structure, which is particularly well visible on the entire surface of the section (Fig. 8C<sub>1</sub>, C<sub>2</sub>). Wider, dark-brown layers are 3.7–4.6 µm thick, whereas thin, transparent and much lighter layers are ca. 1.8 µm wide. Only dark-brown skeletal components stained with acridine-range dye exhibit bright green-yellow fluorescence (Fig. 8C<sub>3</sub>).

## Extant zooxanthellate scleractinians

*Galaxea fascicularis* (Linnaeus, 1767)

**Morphology.**—Septa of *G. fascicularis* show scale-like texture similar to that in *F. chunii* (Fig. 9A, B), however, the pattern of scale-like units arrangement is less regular (“Persian lamb” style) than in *F. chunii* (regular, “roof-tile” style). Scale-like units cover all intracalicular surfaces, and con-

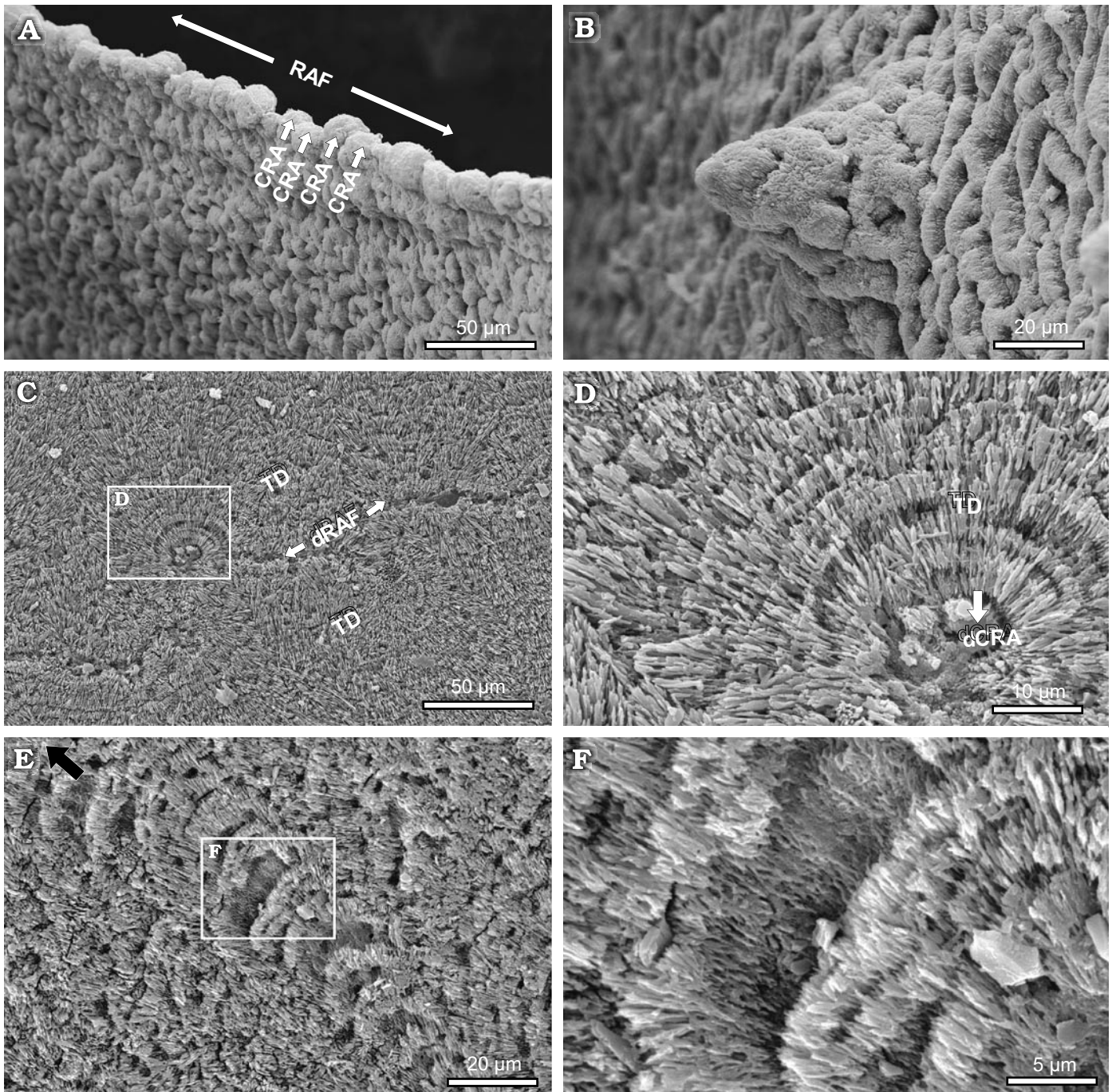


Fig. 9. *Galaxea fascicularis* (Linnaeus, 1767); ZPAL H.23/7 (originally NMNH 90860 lot). Recent, North Pacific Ocean, Central Philippines (southern parts of islands), collection J.B. Steere. **A, B.** Morphology of distal septal edge (**A**) and septal flank spine (**B**). Note “Persian lamb” texture of skeletal surface (as shown by these fasciculi). **C, D.** Transverse section of polished and etched septum. Arrow in enlarged (**D**) fragment (general view in **C**) shows “blurry”, probably organic material in dCRA and adjacent, radiating TD fibers (ca. 3–5  $\mu\text{m}$  growth increments). **E, F.** Septum longitudinally sectioned in RAF plane; note dissolved/etched dRAF components in longitudinal “strand” (**F** enlargement). All are SEM.

tinue on distal, growing edges of skeletal elements in a form of neighboring small tubercles ca. 15  $\mu\text{m}$  across (Fig. 9A).

*Transverse sections.*—Two zones of different light-transparency properties and colors are recognized in transverse section of S1 in TLM (Fig. 10A): (1) dark-brown, partly opaque dRAF zone, and (2) TD zone composed of transparent fibers.

In the central part of the septum, dRAF are bordered with homogenous zone of TD fibers (ca. 10  $\mu\text{m}$  wide). Outwards from this zone, TD fibers show very regular alternations (ca. every 3–5  $\mu\text{m}$ ) of thin darker layers, and slightly thicker, lighter layers (Fig. 10A, red arrows). In the more axial part of this sectioned septum, TD fibers are inclined towards the corallite center (Fig. 10C). Bundles of fibers are gently out-

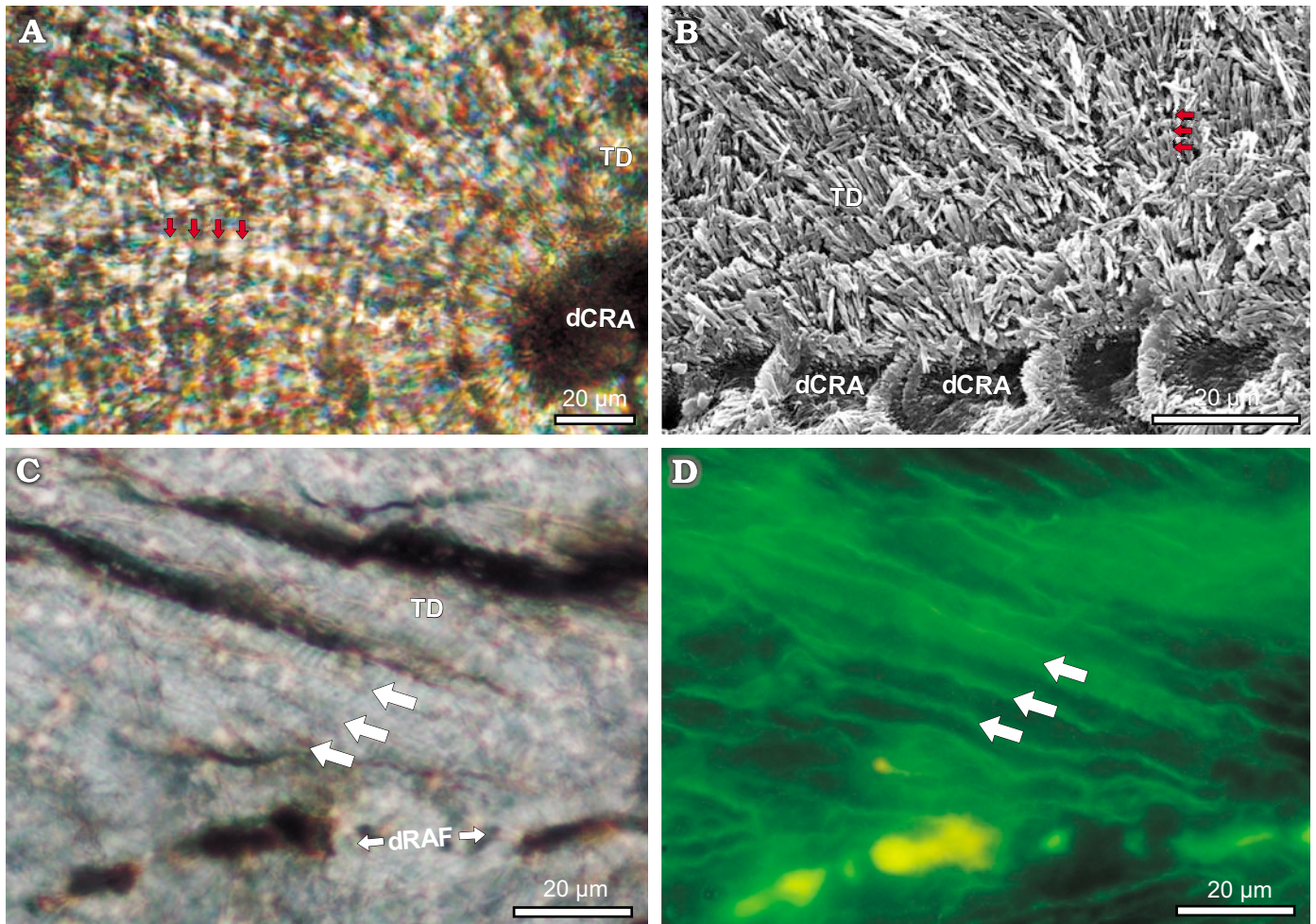


Fig. 10. *Galaxea fascicularis* (Linnaeus, 1767); ZPAL H.23/7 (originally NMNH 90860 lot). Recent, North Pacific Ocean, Central Philippines (southern parts of islands), coll. J.B. Steere. **A.** Transverse polished section of septum in TLM; note dRAF in lower right corner (brown “calcification center”) and regular growth increments of TD fibers (red arrows). **B.** SEM of transverse (slightly oblique) polished and etched section of septum; fibers adjacent to dRAF (bottom) show regular tapering periods at ca. 2–3  $\mu\text{m}$ : red arrows). Oblique sectioned dRAD, with dissolved/etched inner components have crescent appearance. **C.** Transverse polished (slightly oblique) section of septum, TLM view; dRAF show brownish coloration; borders between bundles of fibers only gently outlined (white arrows). **D.** The same septal fragment as C, stained with acridine orange in MFM view; dRAF exhibit light, green-yellow fluorescence, whereas borders between bundles of fibers (arrows) emphasize greenish fluorescence.

lined by brownish borders and similar to the more central part of septum, show regular alternations of darker and lighter layers. In SEM view of polished and lightly-etched section of axial part of septum, dRAF (or distinct dCRA) that have negative etching relief are bordered by crescent-shaped zones of fibers. On both sides of the dRAF zone, bundles of fibers are inclined towards the corallite center and are regularly tapered every 3–5  $\mu\text{m}$  (Fig. 10B, red arrows). In more central part of the septum, dRAF also have negative etching relief (occasionally, with some amorphous material in the center). The only difference with more axial parts of the septum is that bundles of fibers are arranged more perpendicularly to the septal faces (Fig. 9C, D). In MFM view, illustrated in Fig. 10C axial part of septum stained with acridine orange show two zones of different chromatic response (Fig. 10D): dRAF exhibit bright yellow-green fluorescence, whereas borders between bundles of TD fibers show less

prominent, greenish fluorescence. Regular alternations of brownish and more transparent zones viewed within fibers in TLM view (Fig. 10A, and less prominent in Fig. 10C) are not been emphasized in MFM.

*Longitudinal-radial sections.*—Polished and etched sections, made in the septal RAF plane, show regular alternations of regions in SEM, with negative (domed hollows) and positive (ridges) etched relief (Fig. 9E, F). Regions with negative and positive relief alternate approximately every 5  $\mu\text{m}$ , but layers ca. 2–3  $\mu\text{m}$  also have been observed (Fig. 9F).

#### *Platygyra daedalea* (Ellis and Solander, 1786)

A transversely sectioned septum of *P. daedalea* shows in TLM similar zones as *G. fascicularis*, i.e., brownish dRAF (or dCRA if well differentiated) bordered with ca. 10  $\mu\text{m}$  wide zone of TD fibers that further show regular and dense

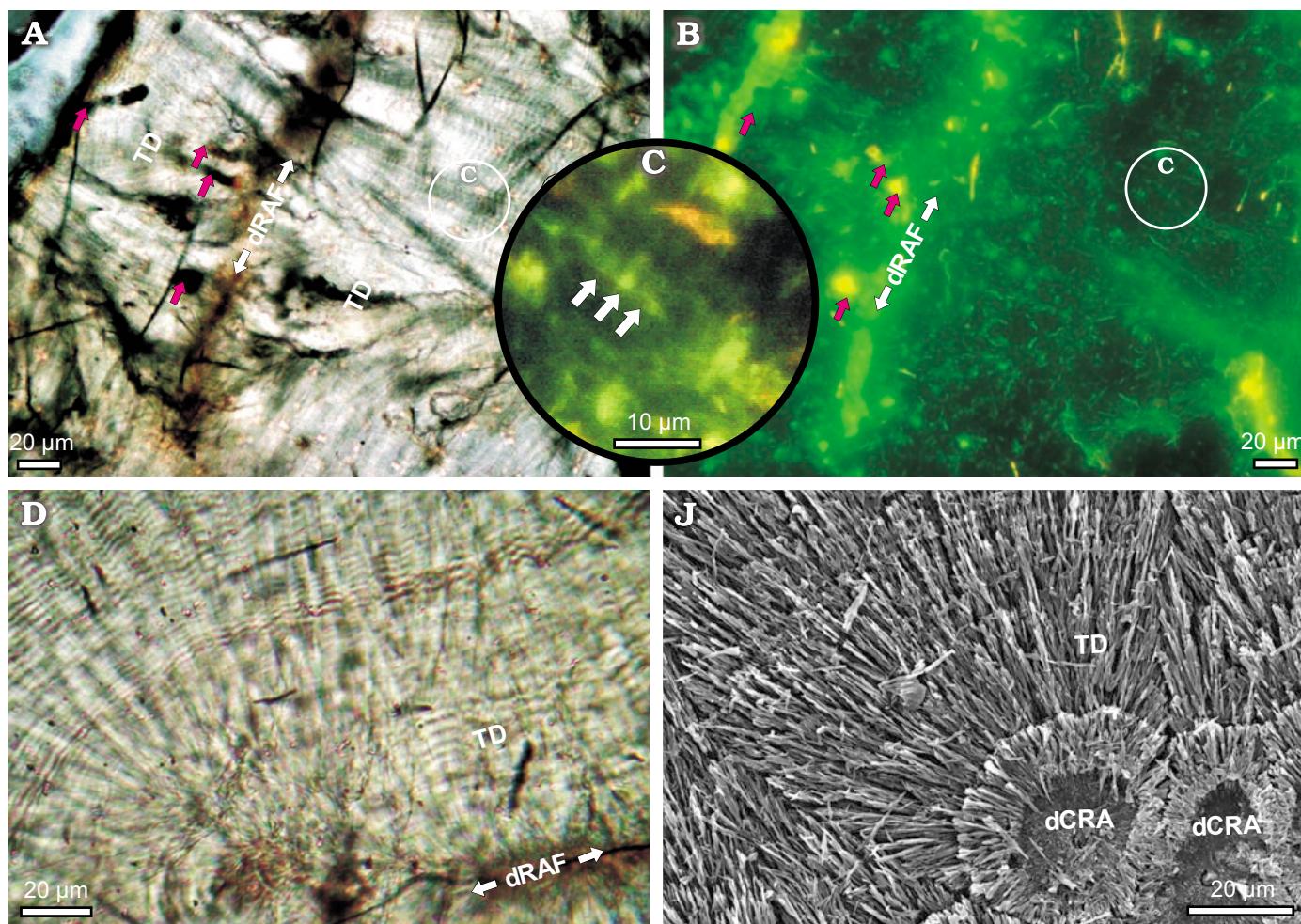


Fig. 11. *Platygyra daedalea* (Ellis and Solander, 1786); ZPAL H.23/8 (originally NMNH A.G. Humes collection. Acc. number 274378). Recent, 25 m, north of Ankazo-beravina, near Nosy Be, Madagascar, August 24, 1967. **A.** Transverse polished section of septum in TLM; note brownish “calcification centers” (dRAF), regular growth increments of fibers (e.g., in encircled area), and dark brown regions (red arrows) of filaments of endolithic organisms (most likely algae, fungi). **B.** The same septal fragment as A, stained with acridine orange in MFM view; dRAF exhibit very light, green-yellow fluorescence; higher magnifications (**C**) show delicate greenish bands matching organic components trapped between successive growth increments of fibers (white arrows). **D.** Transverse polished section of septum in TLM; dRAF in lower right corner; regular growth increments of fibers (TD) are emphasized by levels of brownish bands. **E.** SEM micrograph of transverse polished and etched section of septum; fibers adjacent to row of dRAF (“calcification centers”) taper regularly at ca. 3  $\mu\text{m}$  matching brownish bands in **D**.

alternations (ca. every 3–5  $\mu\text{m}$ ) of thin darker, and slightly thicker, lighter layers (Fig. 11A, D). These alternations are very prominent in TLM, however, darker layers exhibit very weak but recognizable greenish fluorescence in MFM (Fig. 11C). Components of the dRAF zone show much brighter (however not as bright as in *G. fasciularis*) green-yellow fluorescence (Fig. 11B). Dark brown (in TLM) filaments of endolithic organisms (red arrows in Fig. 11A) show bright yellow-green fluorescence in MFM. Scanning electron micrographs of polished and lightly-etched section of the same septal fragment illustrated in Fig. 11D, show oval structures with negative etching relief (dCRA). Outwards from dCRA occurs ca. 10  $\mu\text{m}$  wide zone of fibers. It borders on to the thick zone of TD fibers that are regularly tapered every 3–5  $\mu\text{m}$  or show regular fiber discontinuities between successive layers (Fig. 11E).

## Fossil scleractinians with aragonitic skeletons

Corals chosen in this study came from three different Triassic localities celebrated for preservation of aragonitic corals: Alakir Çay, Turkey (Lower Norian); Dolomites, Italy (Middle Carnian); and Northern Calcareous Alps, Austria (Rhaetian). These are the oldest Mesozoic corals showing exceptional skeleton preservation. Because original aragonitic mineralogy of the investigated samples is preserved (proven by X-ray analysis, Sr contents, see also Scherer 1977), they are suitable for microstructural studies with similar precision as in modern coralla. On the other hand, the depleted amounts of organic components detected in the skeleton of the Triassic *Pachytheclis* by Gautret and Marin

(1993), together with the vestigial fluorescence of acridine orange stained samples seen in this study, clearly indicate that diagenetic alteration affected the primarily organic phase of the skeleton (this conclusion refers also to some “very well preserved” Cenozoic corals as well, see Cuif et al. 1992).

Corals selected herein are traditionally assigned to three main microstructural groups: pachythealliinans, stylophyllinans (“non-trabecular”), and an informal group of “thick-trabecular” corals (Roniewicz 1989; Roniewicz and Morycowa 1993). The focus is on those minute-scale aspects of the skeleton that were observed in modern coralla, i.e.: (1) structure of dRAF zone, especially in longitudinal sections, and (2) regular alternations in TD fibers.

### Unidentified conophylliid

Specimens from Alpe di Specie (Italian Dolomites) that most likely represent a new species of conophylliid have a phaceloid growth form. Coralla have everted calices, which is a common feature of conophylliids; additionally, however, septa have very strongly arched edges hence there is often at least a 90° difference in growth direction between the axial and peripheral parts of septum. Because of such architecture, in transverse section below the convex calice (Fig. 12A), septa in axial part are cut perpendicularly, but in peripheral part longitudinally to their growth. In the peripheral zone of section, septa show mainly fibrous organization, with fibers arranged parallel to the section plane (Fig. 12B). Widely-spaced dCRA occur towards the calicular center (Fig. 12D). In TLM, particularly in peripheral part of septum, fibers show regular (every ca. 5 µm) alternations of thinner, darker layers, and slightly thicker lighter layers (Fig. 12B). In SEM of polished and etched sections of this septal region (Fig. 12C), fibers are regularly tapered every 5 µm, almost identical to zooxanthellate modern corals (compare Figs. 10B, 11E). A longitudinal lightly etched section in dCRA region shows hemispherical, superimposed layers (occasionally >20 µm wide) that in their most convex part are separated by voids caused by preferential etching (Fig. 12E). Distinct borders (negative etching relief) between dCRA layers occur irregularly at 5, 10, and 20 µm intervals.

### *Stylophyllum paradoxum* Frech, 1890

Traditionally, stylophyllinans are considered as non-trabecular corals (Cuif 1973; Beauvais 1982; Roniewicz 1989) i.e., with skeleton built entirely of fibrous sclerenchyme not organized into “continuously growing rods formed by fibers [...], provided with an axis” (clue of trabecula definition in Roniewicz and Stolarski 1999: 165). Contrary to this generalized diagnosis, Stolarski and Russo (2002) suggested that stylophyllids (a major group of stylophyllinans) have skeletons much more microstructurally diversified. There are at least four main microstructural patterns recognized in septal transverse sections; in two of them distinct “centers of calcification” occur (Stolarski and Russo 2002: 662, fig. 11).

Stolarski and Russo (2002) noted that stylophyllid “centers of calcifications” (when present) differ from typical “centers of calcification” of e.g., “thick-trabecular” corals in the lack of a distinct 10–20 µm wide “border layer” (“border layer” is illustrated herein in *Platygyra daedalea*, and *Galaxea fascicularis*—Figs. 10A, 11E). This results in a clear separation of “centers of calcification” from adjacent fibrous parts of the skeleton in non-stylophyllid corals and a lack of this separation in stylophyllids. Herein, more details are given about the skeleton of *Stylophyllum paradoxum* Frech, 1890 included into the 3<sup>rd</sup> microstructural group by Stolarski and Russo (2002). Stylophyllids belonging to this category have single and large “centers of calcification” revealed in transverse sections of septal spines.

*Transverse sections.*—In polished transverse section, in TLM the middle portion of corallum shows a multilayered structure in septal spines. Borders between particular fibrous layers are darker than fibers comprising concentric layers. More central parts of the septal spine (ca. 0.5 mm in diameter) are often differentiated from the outer part of the spine by darker or occasionally lighter appearance (Fig. 13A, B).

*Longitudinal section of septal spine.*—TLM shows that there are several superimposed fibrous layers that comprise the septal spine. In the central part of the spine, crescent zones infilled by spar (ca. 30 µm in width) alternate regularly with typical fibrous layers (ca. 30–40 µm in width)—Fig. 13C–F. Each septal spine includes only one zone with fibrous/spar alternations. Fibrous layers from the central septal spine continue into layers that are thickening the septum (e.g., Fig. 13E, F).

Pachythealliina: *Pachysolenia cylindrica* Cuif, 1975, *Pachytheclis major* Cuif, 1975, and *Zardinophyllum zardini* Montanaro-Galitelli, 1975

Many pachythealliinan skeletal features are unique among skeletonized anthozoans from the earliest Mesozoic, i.e.: (1) a very thick wall (pachythea), the predominant skeletal character has aragonite fibers arranged in penicillate units, which increase centripetally, (2) non-exsert septa, usually located deeply in the calice, and (3) strong bilateral symmetry in initial and juvenile stages (adult coralla may have quasi-radial symmetry), all discussed by Cuif 1975; Stolarski 1999; Roniewicz and Stolarski 2001; Stolarski and Russo 2001. Their skeletal features are, in comparison with other fossil corals, well characterized, although some important microstructural skeletal characters have not been sufficiently well characterized. For example, there are doubts about the microstructure of the narrow pachythealliinan dRAF zone: traditionally septa of all genera are considered non-trabeculate (Cuif 1975), on the other hand Iljina (1984) suggested that in *Pachysolenia* (*P. primorica* Iljina, 1984) they are composed of “trabeculae in series”. The suggestion that separated “centers of calcification” may actually occur in septa of *Pachysolenia* and *Pachytheclis* was recently re-examined by Stolarski and Russo (2001: 245). Another unknown microstructural aspect of the

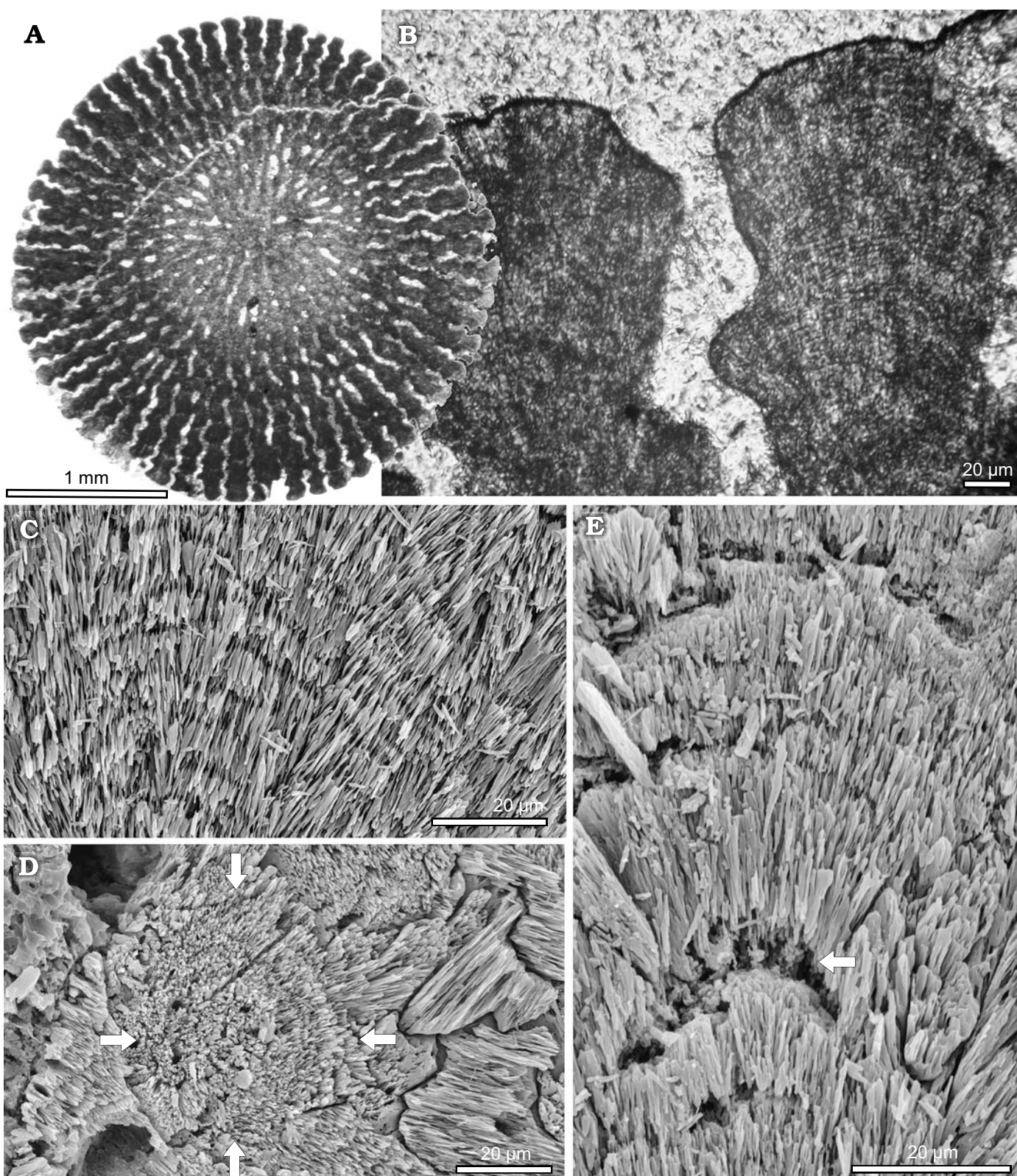


Fig. 12. Undetermined conophylliid. ZPAL H.23/9. Triassic (Middle Carnian), San Cassiano Beds, Alpe di Specie, Dolomiti (Italy), corallum still with aragonitic mineralogy preserved. **B**. Transverse polished section of corallite in TLM (**A**); enlarged portions of longitudinally sectioned septa with regular growth increments of fibers (**B**). **C**. Longitudinally polished and etched section of septum with fibers regularly tapered (SEM). **D**. Transverse, polished and etched septum (SEM) with dCRA ("center of calcification", arrows). **E**. Septum longitudinally sectioned in dCRA region with domed, successive layers of fibers and occasional (arrow) larger voids between them.

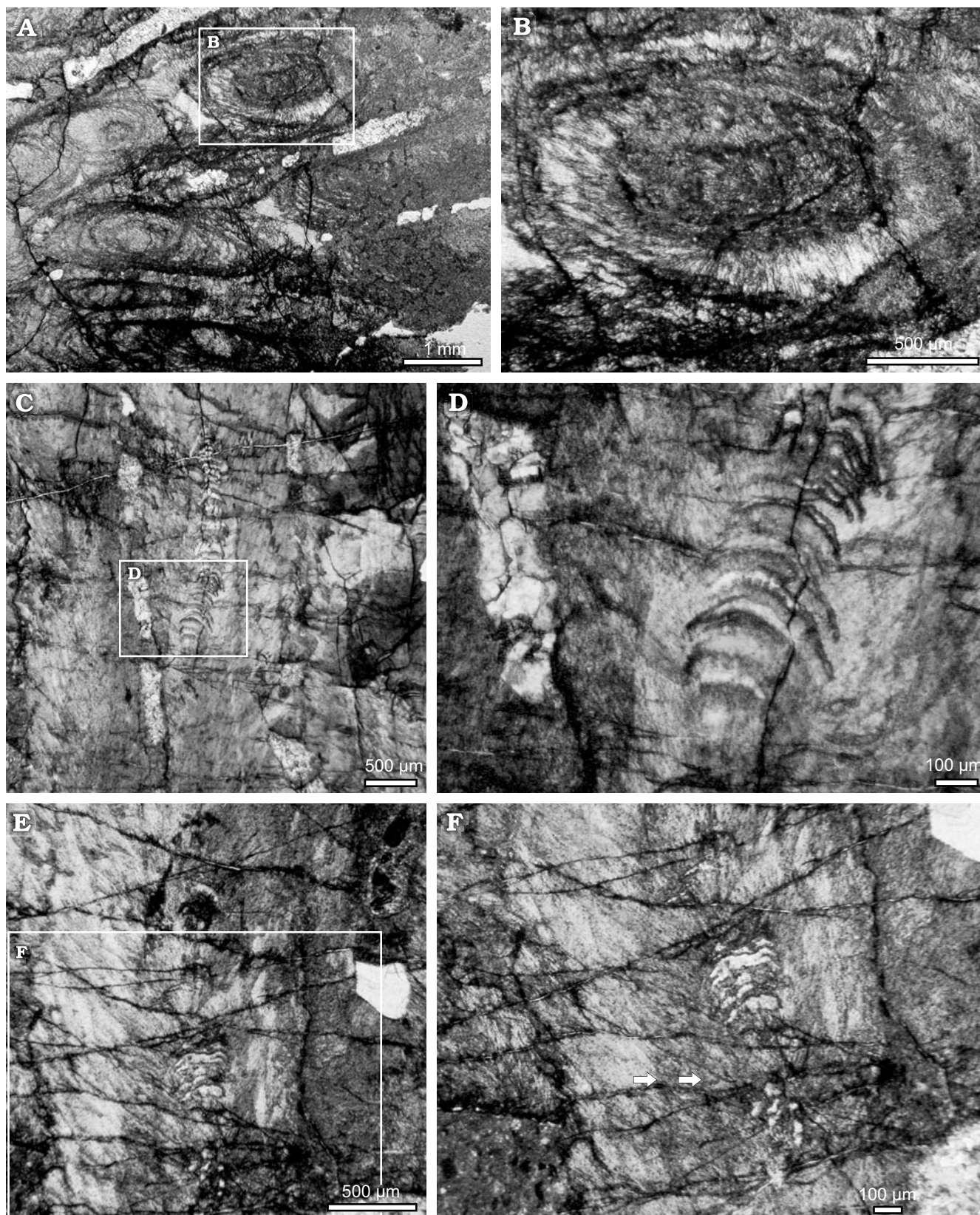


Fig. 13. *Stylophyllum paradoxum* Frech, 1890, NHMW 1982/57/100, corallum with aragonitic mineralogy still preserved. Triassic, Rhaetian, Fischerwiese, Northern Calcareous Alps, Austria. **A, B.** Transverse section of septa with concentric arrangement of fibers within septal spines (**B**, enlargement). **C–F.** Longitudinal sections crossing centers of septal spines; domed, successive layers of aragonite fibers (darker) separated by lighter “voids” infilled by spar (see **D, F** enlargements). Except for regular voids in spine centers, there is no difference in organization of superimposed layers of fibers within septal spine. All TLM micrographs.

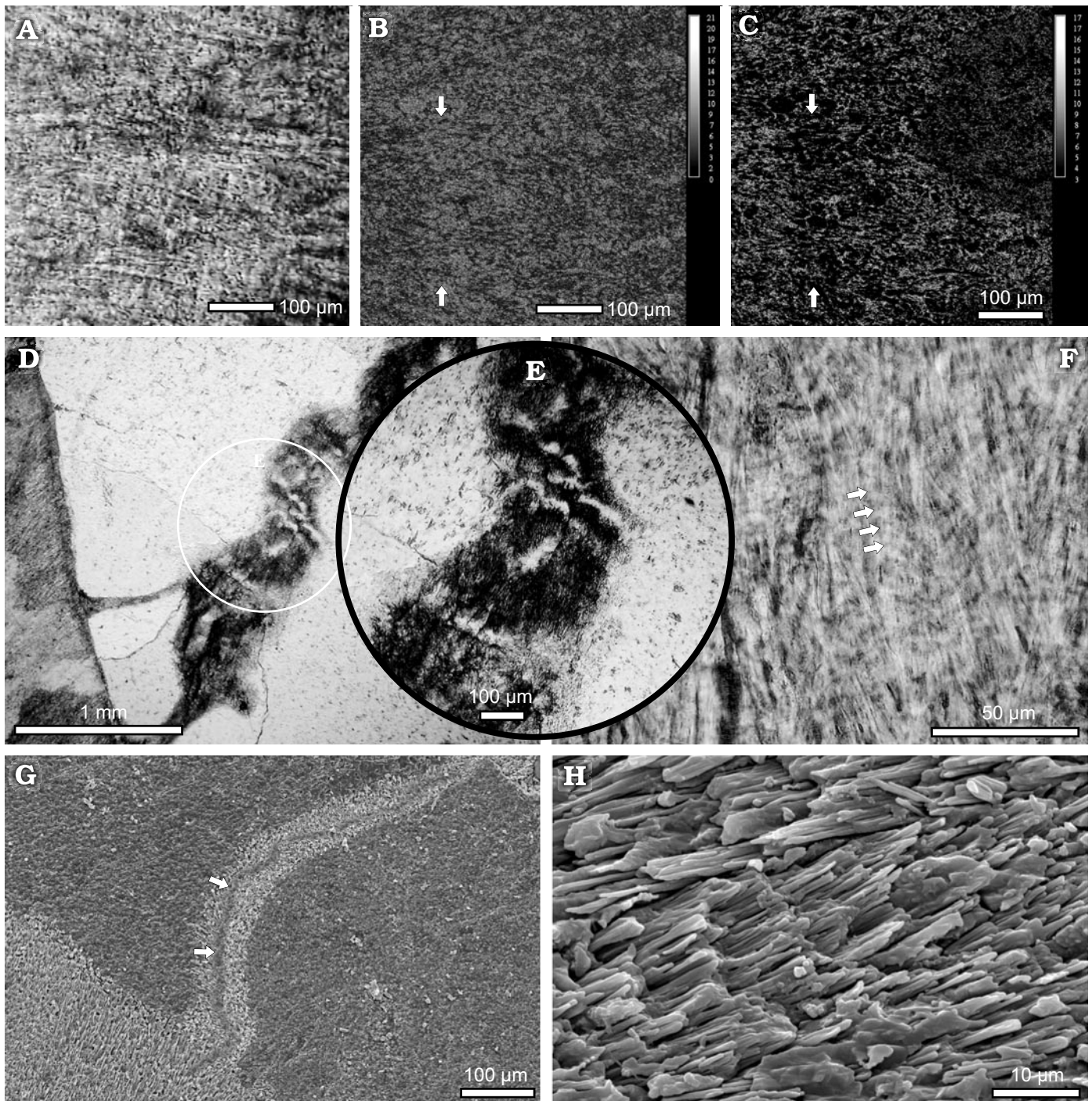


Fig. 14. *Pachysolenia cylindrica* Cuif, 1975, ZPAL H. XXI/4. Triassic, Lower Norian. Alakir Çay, Turkey. **A–C**. Complementary regions of transversely sectioned and polished pachytheca: TLM image (**A**), greyscale Sr (**B**) and Mg (**C**) mapping acquired on the electron microprobe by wavelength-dispersive techniques; darker areas equal very low concentration whereas lighter areas equal slightly higher concentrations. Sr (in **B**) shows enrichment, at least in some regions (arrows) where Mg (in **C**) appears depleted. Sr mapping of diagenetically non-altered fibrous parts of coralla of extant corals (not illustrated here) invariably shows nearly homogenous distribution of this element. **D**. TLM view of longitudinally sectioned pachytheca and septum; part of the preserved septum encircled and enlarged in **E** to show “non-trabecular” nature of dRAF. **F**. Transverse polished section of pachytheca in TLM; fibers show faint regular 5–8 µm alternations of lighter and darker zones. **G**. Homogenous septal dRAF zone in SEM view of transversely polished and etched section. **H**. Transverse polished and etched section of pachytheca (SEM); fibrous skeleton shows negative and positive etching relief (at ca. 5–8 µm distance).

pachytheicaliian skeleton is growth zonation of fibers in pachytheca. Cuif, Dauphin, and Gautret (1999: 591) suggested that in *Pachytheclis major*, the “internal organization

of fibers does not show visible traces of the usual cyclic secretory process”, and later they added that, “obviously, additional aragonitic component has been added during the fossilization

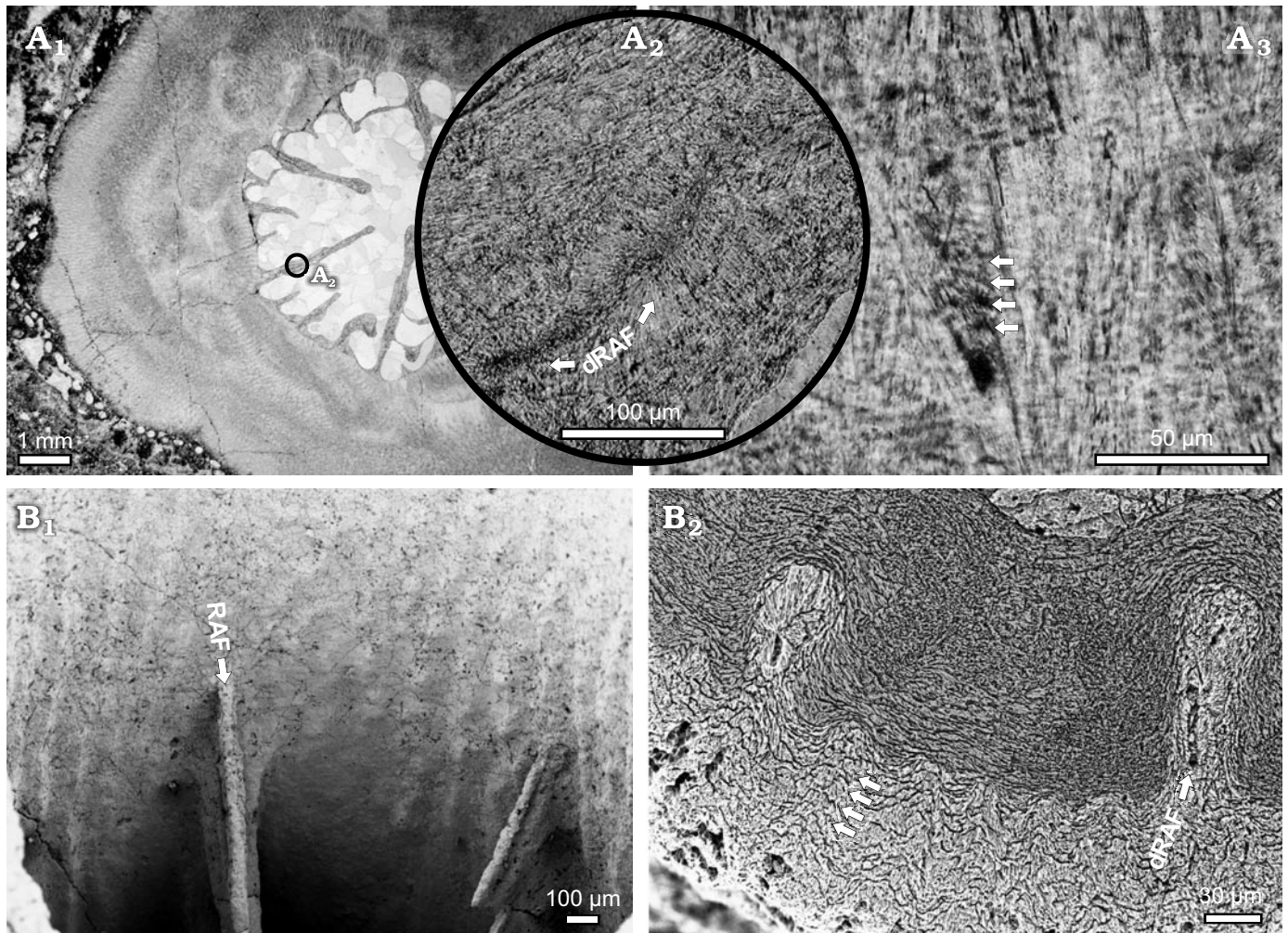


Fig. 15. **A.** *Pachytheccalis major* Cuif, 1975, ZPAL H.23/10. Triassic, Lower Norian. Alakir Çay, Turkey. Transverse polished corallite in TLM (A<sub>1</sub>); enlargement of dRAF (A<sub>2</sub>). A<sub>3</sub>. Transverse polished pachytheca in TLM; fibers show faint regular (ca. 7 µm) alternations of lighter and darker zones. **B.** *Zardinophyllum zardini* Montanaro-Gallitelli, 1975. Triassic (Middle Carnian), San Cassiano Beds, Alpe di Specie, Dolomiti (Italy). Completely smooth RAF of septum in distal view, IPUM11 (B<sub>1</sub>, SEM). B<sub>2</sub>. Transverse, polished and etched septum (ZPAL H.23/11); note fissure in dRAF region (arrow), more or less regular discontinuities in arrangement of pachytheccal fibers (arrows), and secondary, probably biogenic deposits filling up the calice (marked transparent dark grey). All coralla with still preserved aragonitic mineralogy.

process, possibly as syntaxial deposit” (Cuif, Dauphin, and Gautret 1999: 591). However, evidences of regular diagenetic alterations within fossil pachytheccaliinan skeleton have not been provided. The purpose of this work was to supplement observations by previous authors about the original structure of dRAF and pachytheccal TD deposits.

*Pachysolenia cylindrica* Cuif, 1975.—TLM of a transverse section of pachythecca shows bundles of fibers with regular, faint 5–8 µm alternations of lighter and darker zones perpendicular to growth (Fig. 14A, F). In SEM, a polished and etched section of pachythecca (same as viewed in TLM) may occasionally show regions with negative and positive etched relief distributed with a periodicity similar to that seen in TLM for lighter and dark zones. However, in contrast to zones with etched TD fibers regularly tapered e.g., in fossil unidentified conophyllid (Fig. 12C), in *P. cylindrica* negatively etched regions have a “carved” appearance and con-

tinue between larger bundles of fibers (Fig. 14H). Sr and Mg WDS mapping of pachythecca show non-homogenous distribution of these elements (in non-altered aragonite skeletons of extant Scleractinia Sr (and traces of Mg if any) are homogeneously distributed at comparable magnification). In *Pachysolenia*, Sr shows enrichment in regions (arrows in Fig. 14B, C) where Mg appears depleted.

The septal dRAF zone in transverse section viewed in TLM and SEM (Fig. 14G) seems to be homogenous and not differentiated into separate dCRA. The dRAF zone in TLM of longitudinally sectioned septa (which are very thin and undulating) consists of darker bundles of quasi-parallel fibers occasionally separated by “amorphous” and lighter layers (Fig. 14D, E). Fibers are perpendicular to the distal septal margin and not separated by distinct borders as in dRAF zones of extant corals illustrated herein (compare e.g., Figs. 2E, 5C, 6D, 7F).

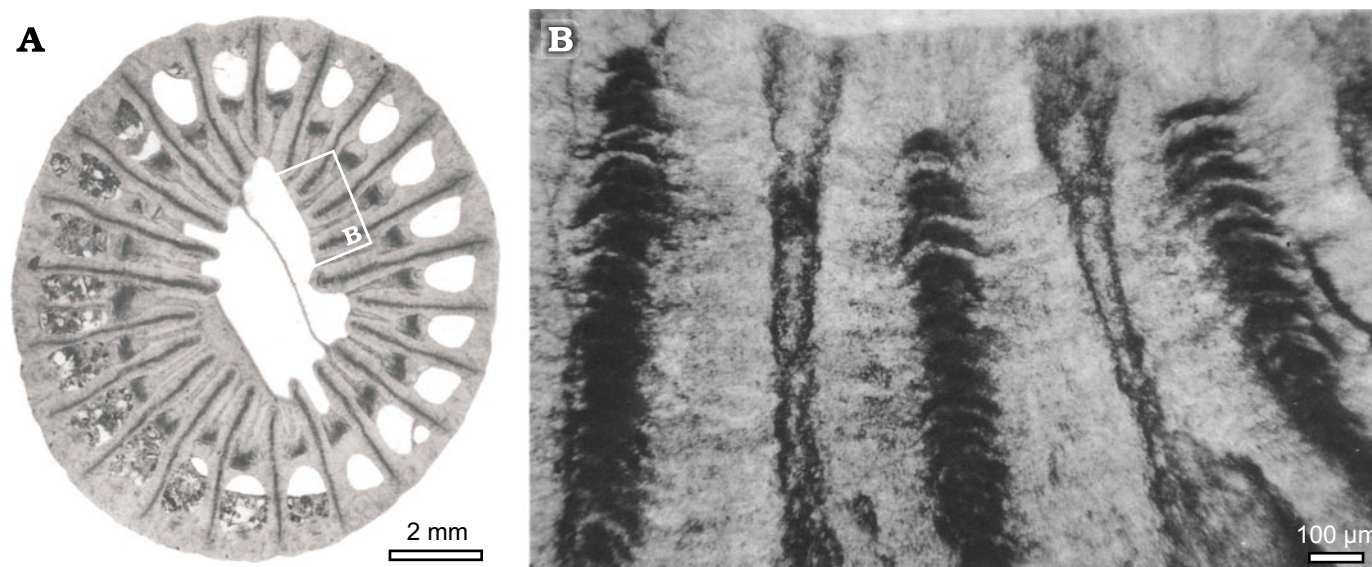


Fig. 16. The rugosan *Endothecium decipiens* Koker, 1924. Here re-illustrated from Schindewolf's (1942: fig. 7). Lower Upper Permian (Basleo-Schichten), Basleo, Timor. "Transverse" section of corallum (A) with septa in axial region (B) showing alternation of layers of fibers (white) and areas infilled by dark (?iron-manganese rich) minerals (see also footnote 2). TLM view.

*Pachytheclis major* Cuif, 1975.—The thick theca of this species, which occurs with *Pachysolenia cylindrica* in the same locality, in transverse, polished section shows faint regular (ca. 7 μm) alternations of lighter and darker zones within bundles of fibers (Fig. 15A<sub>3</sub>). Transverse septal and longitudinal sections through the dRAF zone show the same microstructural organization as in *P. cylindrica*, however, occasionally the homogenous dRAF zone is interrupted and forms elongated and individualized regions (Fig. 15A<sub>1</sub>, A<sub>2</sub>).

*Zardinophyllum zardini* Montanaro-Galitelli, 1975.—This is the only pachytheclian species that occurs in the same locality (Alpe di Specie) as the unidentified conophyllid that preserves extremely faint microstructural details of the skeleton. Similar to other pachytheclianans, *Z. zardini* has smooth septal edges (Fig. 15B<sub>1</sub>). In contrast to specimens from Alakır Çay, Turkey (*Pachysolenia*, *Pachytheclis*), a majority of *Z. zardini* specimens have components of the former dRAF zone removed or possibly dissolved, and this region is easily recognized as a narrow fissure (Fig. 15B<sub>2</sub>). In the few specimens with a solid dRAF zone, it appears to be composed of transparent homogenous material (not differentiated into separate centers) that most likely is secondary infilling. On the other hand, the rest of the skeleton seems very well preserved. Polished and etched bundles of pachytheclia fibers of *Z. zardini*, transverse sections exhibit more or less regular etching banding every ca. 7–10 μm that appears alike the etching pattern of TD fibers in extant corals (Fig. 15B<sub>2</sub>). The "lamellar layer" noted for the first time by Cuif (1975) can also be discerned as a densely layered zone (in contrast to

non-layered sparry calcite in the calicular center) "coating" intracalicular structures, i.e., wall (Fig. 15B<sub>2</sub>).

## Rugosa

A regular two phase arrangement of components within the "dark-line" zone is observed in some rugosans, although detailed comparison is beyond the scope of this paper. Various authors have observed hemispherical structures ("half-moon shaped growth segments" of Weyer 1980) in longitudinal and oblique sections of septa. In the German literature they are referred to "Stirne" and interpreted as the former positions of the septal growth front (Stirnänder of Schindewolf 1942; see also Schouppé and Stacul 1955; Kato 1963: 593 "diffusotrabeular" structure; Schouppé and Stacul 1966; Fedorowski's (1974) correction of the interpretation of Schindewolf and of Schouppé and Stacul; Sorauf and Freiwald 2002). "Stirne" in septa of the Permian species *Endothecium decipiens* Koker, 1924 are here reproduced from Schindewolf (1942: fig. 7). These illustrations (Fig. 16A, B) show the TLM view of septa in the axial region<sup>2</sup> with a regular alternation of fibrous layers (white) and areas infilled by dark (?iron-manganese rich) mineral material. Alternations occur about every 50 μm, hence are more widely separated than organic-enriched and mineral alternations in modern corals described here. On the other hand, they are comparable with bi-phase alternations (every 30–40 μm) in the dRAF zone of the Triassic *Stylophyllum paradoxum* Frech, 1890 (Fig. 13C–F).

<sup>2</sup> Because of the arched shape of the septal growing edge, a "transverse" septal section (as viewed in a central part of the section) often becomes a longitudinal one towards the axial septal region (as also in many modern scleractinians towards the costal region). These geometrical relations explain the hemispherical shape of patches in the dRAF zone in *Endothecium decipiens* and also in modern *Galaxea fascicularis* (Fig. 10B).

## Discussion

Regular mineral-organic alternations of extant coral skeletal components and their spatial distribution in dRAF and TD regions described in this paper provide a basis for reinterpreting the traditional model of corallum formation. The traditional “two-step” model of skeletal growth is compared with the newly proposed “layered” model. The described skeletal structures have potentially significant implications for the taphonomy of fossil coralla and for phylogenetic considerations that integrate skeletal characters.

### “Two-step model”

Details of microscopic structure of coral skeleton revealed by the pioneering works of Koch (1882), Bourne (1887), Frech (1890), Volz (1896), and particularly that of Ogilvie (1897), and these first attempts to use microstructural characters in coral taxonomy, initiated a quest for a general model of skeletal growth. Bryan and Hill's (1942) paper on “spherulitic crystallization” provided a first comprehensive model to explain the underlying processes in coral skeleton formation. The model was based on observations of larger aggregates (spherulites) of calcium carbonate fibers that precipitated in an abiotic environment. According to this model, skeletal growth is initiated “at certain points of ectoderm” i.e., “centers of calcification” (1), where “more concentrated production of the calcareous gel take place.” Once initiated, further growth of fibers (2) continues “automatically and along predictable lines”, each fiber being a “single orthorhombic crystal of aragonite”. This growth results in the formation of “axiolytic type” spherulitic structures, i.e., trabeculae, each being “a cylinder tapering convexly at the top, and consisting of fibres, usually curved, directed upwards and outwards from a common axis” (Bryan and Hill 1942: 79). Bryan and Hill (1942: 80) suggested that “‘darkening’ at the axes of trabeculae (...) appears to be due to excessively finely divided matter interstitial to the fibres at these places”. They noticed also “delicate and remarkably regular alternations” of fibers (p. 88), however they did not comment on this phenomenon, formerly observed only by Ogilvie (1897).

This mineralogical-based model gained general acceptance, especially among paleontologists. Trabeculae seen in variously oriented sections came to be characterized by their shape, diameter, number and arrangement of “centers of calcification” (see reviews in Wells 1956, and Roniewicz 1996). Trabecular dimensions became important diagnostic characters of suprageneric taxa: e.g., Alloiteau (1957) noticed that in Caryophylliidae, Aphiastraedidae, and Turbinoliidae that trabeculae are 0.01–0.015 mm in diameter whereas in *Pseudoseris* they reach 0.5 mm; according to Kato (1963) trabeculae in *Rugosa* are about 0.1–0.5 mm in diameter. Roniewicz and

Morycowa (1993) proposed a four-fold higher-level classification of Scleractinia which distinguished trabeculae-based taxonomic categories. These are: (1) “minitrabecular” corals with very small trabeculae (20 to 50  $\mu\text{m}$  in diameter), (2) “thick-trabecular” corals with medium-sized (50–100  $\mu\text{m}$ ) and large-size (100–1000  $\mu\text{m}$ ) trabeculae, (3) “fascicular” (= stylophyllinans) corals without typical trabeculae, and (4) pachythecaliinans, the only group characterized by its wall type and not by features of septal trabeculae.

Despite the seemingly clear definition of trabecula and the immense number of publications in which this term was used, in many cases, especially in “thick-trabecular corals”, the decision where to set the boundary between trabeculae and fibrous tissue that successively thickens skeletal structures (stereome) proved arbitrary. This problem was skillfully sidestepped by Roniewicz (1989), who interpolated trabecular dimensions by measuring distances between neighboring “centers of calcification” (along “mid-septal” zone in transverse sections) or between distinct borders of fibers (in longitudinal-radial sections of septa). However, Cuif et al. (1997) considered the geometric aspects of “trabecula” to be of little phylogenetic value, focusing instead on the profound microstructural and biochemical differences between “centers of calcification” (= trabecular axes) and fibers (= trabecular fibers + stereome). In their significantly updated two-step model, a crucial role is played by “centers of calcification” composed of “tiny crystals (size 1 micron), densely packed, rather randomly oriented, and surrounded by electron diffuse reflecting material”, hence most likely embedded in an organic material (Cuif and Dauphin 1998: 264). Cuif and Sorauf (2001: 148) noticed that occasionally “centers of calcification” appear to be wholly organic, but when a mineral phase exists “the small crystals [...] are invariably aragonite”; a conclusion contradicting Constantz and Meike's (1990) suggestion about the calcitic mineralogy of minute crystals. The concept of fibers has also been significantly amended by showing that they are not “single orthorhombic crystals” (Bryan and Hill 1940) but composite structures with very fine organomineral alternation that suggest several successive growth steps (Cuif et al. 1987). Cuif et al. (1997) questioned the function of “centers of calcification” as sites inducing crystallization of aragonite fibers by showing separation of both structures on the most distal growth edges of skeletal structures and transverse sections. This led to the reinterpretation of “centers of calcification” as deposited in the first growth phase and whose main function is to serve as scaffolding for continued growth of successive fibrous layers, thus determining the shape of the skeleton (see summary by Cuif and Sorauf 2001). Symptomatically, because of former mineralogical connotations, the term “calcification center” has been nearly always used in quotation marks (e.g., Cuif et al. 1997<sup>3</sup>). This inadequacy has recently been addressed by Cuif, Dauphin, et al.

<sup>3</sup> Wells (1956) also recognized the unclear terminology of “centers of calcification” and consistently used this term in quotation marks. A purely mineralogical function was attributed to “centers of calcification” by Wainwright (1964) who considered their dark coloration a result of the lack of optical orientation of micron-sized crystals. Constantz (1986a, b) also considered them “seeds” for the crystallization of aragonitic fibers.

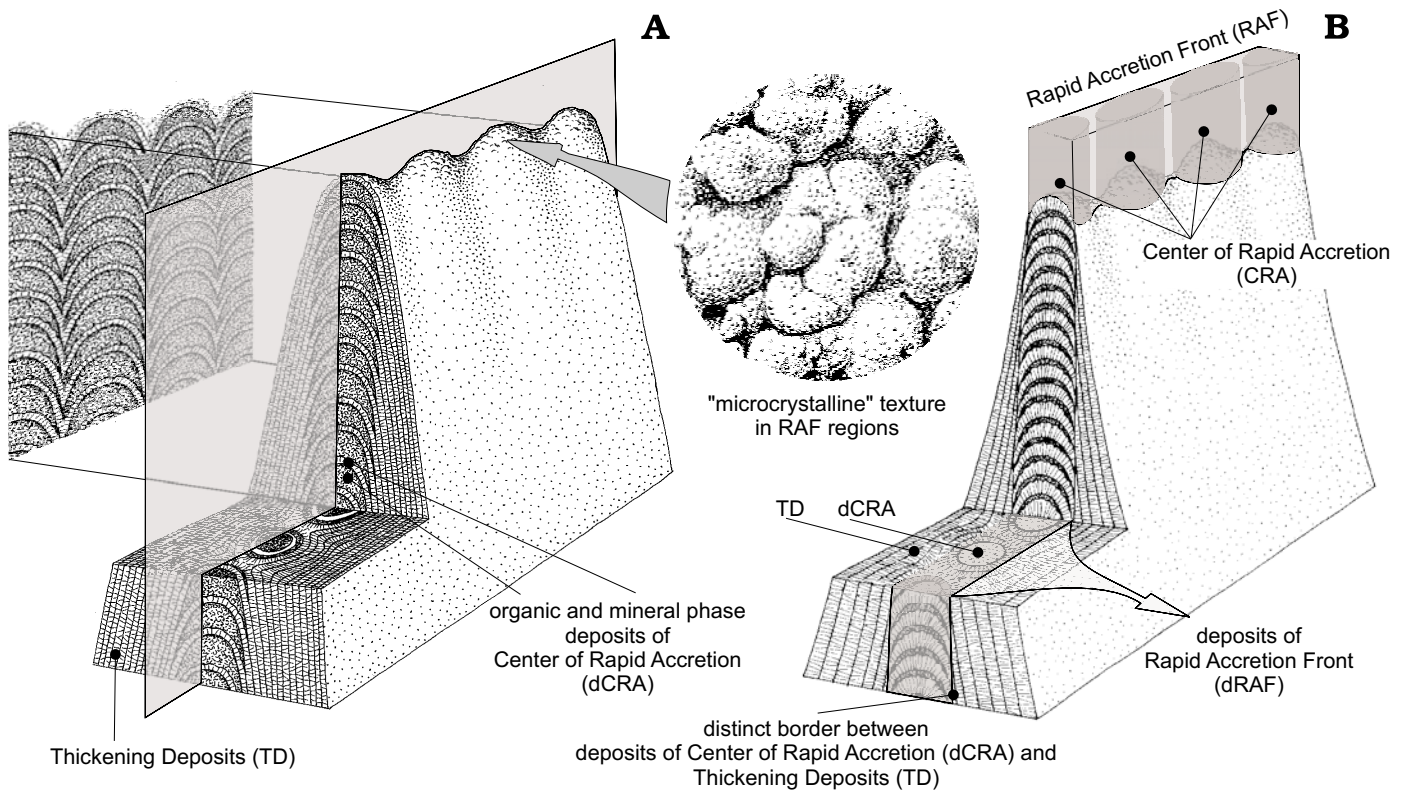


Fig. 17. Idealized and representing two extremes, three-dimensional models of septal microstructures in corals with fibrous skeletal tissue. First extreme model (A), shows perfect continuity between organo-mineral phases of dRAF and TD regions, whereas the second extreme model (B) shows consistent discontinuity of these phases in longitudinal, perpendicular to septal plane section. Real specimens (e.g., Figs. 3E–H, 5B) usually have some regions with dRAF and TD layers continuing, and some parts where these layers discontinue. Left to A, longitudinal section through RAF plane. Septal surfaces in the RAF zone may have “microcrystalline” texture (if a snapshot were taken during formation of the mineral phase); “microcrystals” represent exposed fiber tips (fasciculi of Wise 1972) of organic-depleted zones (circle on right of A).

(2003), who proposed the “Early Mineralization Zone (EMZ)”. This perfectly fits the modified “two-step” model: it clearly points to temporal differences in the formation of structurally and biochemically distinct skeletal components.

### “Layered model”

The two-step model and concept of an Early Mineralization Zone (Cuif, Dauphin et al. 2003) emphasize differences in the time of formation of “centers of calcification” and fibers. However, as shown here, continuity of layers of aragonitic fibers at least in some directions, between these regions (e.g., Figs. 3E–H, 5B) clearly suggests the fibers and “centers of calcification” having in part formed simultaneously. Differences between “elevated” RAF and “depressed” TD regions can be better ascribed to different growth dynamics, rather than differences in timing, and this is proposed in the “layered model”. The “layered model” predicts that steady skeleton growth results in formation of TD i.e., continuous and superimposed fibrous layers (e.g., flat regions of the basal plate, smooth septal faces, etc.). On the other hand, increased skeletal growth of centers (CRA) or linear regions (RAF) results in the formation of dCRA/dRAF with much higher content of organic-enriched

components in comparison to their limited amount in TD regions. This suggests that boosting of growth is attained mainly by increased production of organic phases and not mineral phases. Though the boundary between RAF and TD regions is gradational in terms of the mineral phases, it is well defined by organic phase characteristics. More detailed description of the two regions is provided below.

### *Deposits of the Rapid Accretion Front (dRAF)*

Some of the observations that form the basis of the conclusions of this paper, have been noted previously, though they have been largely ignored in modern biomineralization literature. For example, the alternating nature of the “trabecular axes” was documented in longitudinal sections by Wise et al. (1970), Wise (1972), Jell (1974), and Jell and Hill (1974), although their organo-mineral nature was not proven. Wise (1972: 163) described that in the “trabecular axis” of *Mycetophyllia* “growth banding is quite prominent, and the dark, more heavily etched portions appear to represent areas of finer crystal size and very possibly areas of higher organic content” (however, finer crystals have not been shown). Jell (1974: 308) observed in radial longitudinal section of “trabecular axis” of *Fungia scutaria* a “row of small hemispherical areas [...] bounded upwards by a thin layer of small tufts 1.5 to 2.0 microns in width. In etched

surfaces the areas below this rim are depressions". These depressions "may represent areas of concentration of organic material or alternatively, the areas of crystals seeding by which there is an aggregation of crystals very much smaller than those in the tufts" Jell (1974: 316). Jell (1974: 7d, 1975: pl. 2: 1) also illustrated clearly, that layers with negative and positive etching relief superimpose and continue smoothly outside the most convex part of dRAF, however, in the same direction, the thickness of zone with negative etching relief (i.e., as proved herein, enriched in organic components) reduces significantly.

MFM (organic components stained with acridine orange dye), TLM, SEM (etched samples) observations of organo-mineral alternations in the skeleton of modern corals, support Jell's (1974) suggestion about enrichment in organic components of those regions that have dark brown color in TLM and negative relief in etched sections (SEM). Organic-enriched dRAF regions are lens- or dome-shaped and separated by thin mineral layers. In longitudinal sections perpendicular to the septum (Fig. 3F–H), regions with negative etching relief (= organic) continue as a very thin zone separating successive mineral layers outside the most convex part of dRAF. In this study, the regular dRAF zone, composed of alternating organo-mineral components, was also identified in *Stephanocyathus paliferus* (e.g., Figs. 2B, F, 3C, D), *Flabellum chunii* (e.g., Figs. 5C<sub>2</sub>, 6D), "*Ceratotrochus*" *magnaghii* (Fig. 8C), *Galaxea fascicularis* (Fig. 9E, F). Also "strands" in *Desmophyllum dianthus* dRAF show fine regular constrictions that suggest similar organo-mineral alternations, though the organic-phase may dominate. In longitudinal-radial sections of corals with nearly completely smooth septal edges (no distinct CRA), layers enriched in organic components may continue between neighboring dRAF "strands" (Figs. 2E, 8C). On the other hand, in other regions of the same section, but especially in corals with clearly separated but closely spaced CRA (appearing as protuberances on distal edge; Figs. 9A, 17), organo-mineral layers are separated within each "strand" (in longitudinal-radial section).

Successive thin layers of dRAF mineral phase that enclose organic lens-shaped layers are composed of short but not isometric aragonite fibers, usually ca. 1.5–5  $\mu\text{m}$  in length (e.g., Figs. 3C, D, 5B, C<sub>2</sub>, 9E, F). The interpretation that the basic components of "centers of calcification" are isometric aragonitic crystals (e.g., Wainwright 1963) has persisted in the paleontological literature for so long possibly because most of observations were made on septal distal tips or transverse sections. It is worth noting that the multilayered structure of the skeleton occasionally observed in transverse sections (herein Fig. 5D<sub>2</sub>, or e.g., Cuif and Dauphin 1998: fig. 3.3) can be best explained as dome-shaped organo-mineral alternations. However, nanogranular, possibly isometric material was observed in the RAF plane of unetched, polished sections of *Stephanocyathus paliferus*. Granular material, exposed in shallow grooves that correspond to organic-enriched dRAF regions, is made up of particles about 50 nm in diameter (Fig. 4D, E). The shallow grooves were produced either by dissolution of organic components during polishing or by selective grinding of

softer organics, leaving a nondissolved or harder residuum. It is noteworthy that Clode and Marshall (2003a) showed nanocrystals (the smallest ca. 20 nm in diameter, and the largest were about 400 nm in diameter) on denticles at the apices of exsert septa of *Galaxea fascicularis* and on the septa of the axial corallite of *Acropora formosa*. These authors suggested that the deposition of nanocrystals may be the surface manifestation of centers of calcification. On the other hand, preliminary AFM observations of "flat" surfaces bordering on grooves have texture with similar ca. 50 nm granules. One may only speculate that 50 nm particles are basic components of the entire skeleton mineral phase, hence are not limited to dRAF regions (see also chapter: Physiological control upon skeleton formation).

The essence of the "layered model" is that mineral layers that originate in the center of dRAF continue in some directions into the TD region. An ideal version of this model is shown in Fig. 17A. Nonetheless, such a perfect arrangement of layers has never been observed: layers may discontinue shortly after passing from the dRAF region to the lateral (TD) flank of the septum, or may develop asymmetrically on septum sides, etc. Theoretically, if the growth rate in RAF regions would significantly exceed that of TD, this would result in a discontinuity between dRAF and TD and development of two structurally independent regions as in the "two-step" model. However, this has not been observed in the material studied and the model illustrated in Fig. 17B is hypothetical (thus, if confirmed, the "two-step" model would be a particular case of the "layered model"). Possibly other necessary "adjustments" of the proposed "layered model" will be necessary to encompass various "unorthodox" biomineralization patterns, e.g., corals with "scale-like" skeleton (e.g., acroporids).

#### *Thickening Deposits (TD)*

The TD region, in comparison with dRAF, is significantly depleted in organic-enriched components. Nevertheless, TD organic components are recognized by their brownish coloration in TLM and green-orange or green-yellow fluorescence in MFM, and show the following distribution patterns: (1) narrow "bumpy" layers between aragonitic layers and individual bundles of fibers (e.g., regions of green-orange fluorescence in *Stephanocyathus paliferus*, Fig. 2D); (2) a compact, densely banded zone enclosing septal and wall dRAF and a loose network of narrow layers between bundles of fibers and/or apparent fractures (green-yellow and respectively, orange-green fluorescence in *Desmophyllum dianthus* Fig. 7E); (3) distinct, narrow layers parallel to bundles of fibers (oblique to septal surface in axial region, greenish fluorescence in *Galaxea fascicularis* Fig. 10D); (4) non-distinct, poorly visible narrow layers between individual bundles of fibers showing very weak greenish fluorescence of organic components trapped between successive growth increments of fibers (*Platygyra daedalea*, Fig. 11B).

Overall, TD organic components appear much weaker and occasionally differ in color (green-orange, or reddish Gautret et al. 2000: fig. 1E, F) fluorescence intensity relative to dRAF

regions; many produce an alteration in the emission spectrum suggesting different biochemical properties (changes in pH, binding of the fluorophore to specific ions, etc.), however, determination of biochemical composition of dRAF and TD components is beyond the scope of this paper.

TD layers of zooxanthellate and azooxanthellate corals generally show small growth increments (a few micrometers in width) marked by organo-mineral alternations. However, these alternations differ significantly between corals from both ecological groups. In transverse sections of zooxanthellate *Galaxea*, *Platygyra* (also not illustrated *Hydnophora* and *Favia*), alternations are very regular, borders are very distinct and easily detected in TLM (Figs. 10A, B, 11A–E), whereas in azooxanthellate corals they never form such a regular and perceptible pattern as seen in zooxanthellate corals (Figs. 3A, 7A, 8B). Further microstructural and TLM studies are needed to identify discernible and robust criteria for discriminating between zooxanthellate and non-zooxanthellate corals. If found, they will have far-reaching consequences, because such skeletal criteria can also be preserved in fossil coralla. The first candidate of fossil zooxanthellate coral that should be examined using such criteria should be the unidentified conophyllid, where aragonitic fibers show very regular alternations in TLM and SEM (Fig. 12B, C).

## Physiological and environmental control of the skeletal growth

This chapter compares various “minute-scale” aspects of the “layered model” with physiological data, *in vitro* observations of skeletal growth, and histological observations of the nearly intact tissue/skeleton interface gathered from the literature. The initial focus is on the initiation of skeletogenesis; skeletal components formed during these processes appear similar to micro- and nanostructural components observed here in dRAF regions. This is followed by a review of the processes of rhythmic growth that operate on various scales and may cause different patterns of fiber alternations between zooxanthellate and azooxanthellate corals.

### *Initiation of skeletogenesis*

Hayes and Goreau (1977a, b), and Goreau and Hayes (1977) considered that calcicoblastic ectoderm cells produce skeletal precursors, i.e., aragonite crystal-bearing vesicles that provide seed-crystals and organic matrix into the sub-epithelial space. Subsequently, Isa (1986) regarded calcium-rich spherules found in sub-epithelial space of osmicated tissue from *Acropora hebes* as precursors of 50 nm aragonite granulae and sites of initial nucleation. Johnston (1980) distinguished two regions where the main organic components were involved in skeletal formation: (1) a ca. 3  $\mu\text{m}$  thick meshwork of tiny (0.1–0.3  $\mu\text{m}$  wide) compartments penetrating into the skeleton up to 10  $\mu\text{m}$  from the growth surface in the fastest growing skeletal portions and only 1  $\mu\text{m}$  in the slower growing portions); (2) larger organic sheets or lamellae, serially arranged to form a series of chambers ca. 4  $\mu\text{m}$  in diameter that delineate

bundles of fibers in deeper areas of the skeleton. Clode and Marshall (2002), using frozen-hydrated (FZ) preparative techniques for FESEM observations, challenged some of these former interpretations, concluding that vesicular exocytosis of precursor organic matrix material seen in chemically fixed preparates (also by Johnston 1980; Yamashiro and Samata 1996; Goldberg 2001) was caused by preparation artefacts. However, similar to Johnston (1980), Clode and Marshall (2002, 2003b) observed a mesh-like network of fibrillar (ca. 26 nm in diameter) organic matrix at the calcifying interface penetrating between aragonitic crystals and extending to calcicoblastic cells. Nodular structures (23–48 nm in diameter:  $37 \pm 2$  nm on average) that were randomly distributed on individual fibrils have been considered nascent calcium carbonate crystals (Clode and Marshall 2003b).

*In vitro* studies by Domart-Coulon et al. (2001) of primary multicellular cultures isolated from fast-growing apical colony fragments of *Pocillopora damicornis* showed the presence of aragonitic carbonate nodules (5–20  $\mu\text{m}$  in diameter if spherical, or 20  $\mu\text{m}$  if elongated) within adherent multicellular isolates. These nodules appeared to be composed of 50 nm to 1  $\mu\text{m}$  long rod-shaped aragonite grains, each containing numerous nanocrystalline domains.

These two lines of evidence, i.e., from histology of skeletal-tissue interface (Clode and Marshall 2003b) and from isolated cell cultures (Domart-Coulon et al. 2001), suggest that nascent calcium carbonate crystals in corals are nanocrystalline, i.e., ca. 50 nm in size. Thus, one may speculate that the 50 nm granulae observed in dRAF zone of *Stephanocyathus paliferus* are actually incipient skeletal units used in further skeletogenesis. In the dRAF region these crystals are probably embedded in the abundant organic phase and hence are particularly easily discernible. On the other hand, similar nanogranular textures of some other skeletal regions hint that such nanocomponents may be a part of the whole skeleton. Interestingly, similar, ca. 40–50 nm randomly oriented granulae were observed in the etched fibrillar crystallites of cephalopod shells (*Nautilus*, *Spirula*) by Dauphin (2001), while Grégoire (1987) noted similar nodular structures upon the organic matrix of *Nautilus pompilius*; this suggests the existence of some more general biochemical constraints on the formation of nascent crystals.

The differentiation of skeletal regions into RAF and TD and the enhanced growth in RAF zone, as proposed by “layered model”, suggest that significant physiological changes have to occur in the skeletogenic cells. Indirect support for this thesis is provided by Le Tissier (1991) who described two cellular domains in the skeletogenic part of the basal ectoderm: (1) thin, with highly interdigitated lateral cell borders and prominent intracellular spaces in places of active skeletal deposition (?RAF), (2) thick, without interdigitated lateral cell borders in places of less active skeleton deposition (?TD).

### *Growth periodicity*

A striking feature of all examined coralla is the growth periodicity of dRAF and TD. As seen in TLM, these appear as

$\mu\text{m}$ -scale alternating layers of transparent, nearly colorless material, and darker, slightly more opaque layers with brownish coloration. Optically different phases correspond to alternations of fluorescing organic-enriched phases (preferentially etched) and phases lacking fluorescence response (more resistant to etching); Figs. 2B, E, F, 10A, 11A, D. Since growth periodicity of zooxanthellate and azooxanthellate corals (i.e., living with *versus* lacking symbiotic, photosynthesizing algae) is constrained by different physiological and environmental factors, they are discussed separately.

*Zooxanthellate corals*.—Skeletal density bands that correlate with annual or other seasonal cyclic events provide means to estimate age and growth rates of living and fossil corals (for overview of an extensive literature, visit <http://www.aims.gov.au/pages/auscore/auscore-08.html>). A flurry of publications dealing with much finer, micro-scale banding that occur within wider seasonal/annual bands in zooxanthellate corals dates back to Wells (1963)<sup>4</sup> who interpreted fine epithecal wrinkles as representing daily increments and showed their practical use for geochronometric assessments. A diurnal rhythm of epitheca formation, reflecting daily changes in the shape of secreting tissues, was experimentally confirmed by Barnes (1972). Further, extensive studies of coral calcification outlined the complex background of day-night differences in calcification of zooxanthellate corals.

Some studies suggest distinct differences in day-night calcification growth rates and in formation of distinct crystalline structures. For example, Barnes and Crossland (1980) and Strömberg (1987) showed that the night rate of skeleton extension (but not overall calcification) of *Acropora* is equal to or greater (up to 20%) to that occurring during the day (range of 24-h period extension 0.1–0.5 mm). Gladfelter (1982, 1983) observed the formation of two distinct skeletal components in *Acropora cervicornis*, (1) fusiform crystals (ca. 2–3  $\mu\text{m}$  long) during nighttime hours on skeletal growth edges, and (2) needle-like, epitaxially growing crystals on the surface of the previously formed fusiform crystal framework during daytime hours<sup>5</sup>. Similar diurnal patterns of crystal formation were described by Le Tissier (1988) in *Pocillopora damicornis*: fusiform crystals (0.5  $\mu\text{m}$  long) deposited at skeletal apical spines (forming fasciculi) during the night *versus* needle-like crystals formed during the day.

On the other hand, differences in day-night calcification need not be marked by deposition of fusiform vs. needle-like crystals. In temperate *Plesiastrea versipora* (Lamarck, 1816) in light,  $\text{CaCO}_3$  is deposited as small spheroidal crystals and, at higher temperatures, small needle-shaped crystals, whereas

in the dark, as amorphous sheet-like cements (Howe and Marshall 2002). Also, in corals that form fusiform crystals their deposition may not be restricted to the night: at the growing septal edges of *Galaxea fascicularis* they were deposited continuously without apparent diurnal change (Hidaka 1991a, b; Clode and Marshall 2003a). In the latter coral, intense calcification occurs in the dark, specifically at exsert septa (growing corallite edges), whereas in the light it takes place both at growing edges and other (wall) skeletal elements (Marshall and Wright 1998; Clode and Marshall 2003b). Fast growing, exsert septa of *G. fascicularis* are covered with tissue devoid of zooxanthellae hence, according to Marshall (1996), their calcification is not dark-repressed in comparison to other skeletal parts formed in the vicinity of photosynthetic algae (the same mechanism was suggested to explain faster growth rate of the axial corallites of *Acropora*, see Marshall 1996).

In addition to differences in secretory activity and anatomical conformation that may leave a distinct diurnal signal in skeletal macro- and microstructures, there is diverse evidence for diurnal rhythms involving polyps' physiology and the histology of their tissue. Le Tissier (1988) demonstrated that in *Pocillopora damicornis* during the night, calcicoblastic ectoderm of overlying apical spines was much thicker than that overlying non-apical skeletal elements and showed a greater degree of cellular activity. A number of hypotheses have been put forth to explain whether and (if so) why, calcification should be enhanced by daily photosynthetic activity of zooxanthellae (papers following the pioneering research by Goreau 1959 are reviewed in Barnes and Chalker 1990, see also Allemand et al. 1998; McConnaughey 1989; McConnaughey and Whelan 1997; and Marshall and Clode 2002). Recently, Al-Horani et al (2003) using  $\text{Ca}^{2+}$ , pH, and  $\text{O}_2$  micro-sensors to measure basic photosynthetic and calcification parameters in three body compartments, suggested that high rates of calcification in light are favored by coupled Ca-ATPase transport of  $\text{Ca}^{2+}$  to the calcifying sites and removal of protons produced in the calcification reaction ( $\text{CaATP Ca}^{2+} + \text{H}_2\text{O} + \text{CO}_2 \rightarrow \text{CaCO}_3 + 2\text{H}^+$ ). The result is an increase of pH, thereby increasing supersaturation of aragonite under the calcicoblastic layer. On the other hand (as indicated in the paragraph above), Marshall (1996) favoured McConnaughey's (1989) model, thus implying that it is calcification that enhances photosynthesis. He observed that in zooxanthellate corals, night calcification is repressed (except for sites lacking zooxanthellae, i.e., exsert septa) whereas azooxanthellate corals calcify at more or less constant rates.

We still do not have a comprehensive model to explain the chain of causal influences of day-night biochemical and physiological cycles on composition and distribution of organic ma-

<sup>4</sup> In fact, Bryan and Hill (1942: 88) had already suggested a diurnal rhythm in skeletal growth that resulted from a "pulsation in the supply of  $\text{CaCO}_3$ ", pointing out that a "majority of corals are closed and quiescent during the day, and are expanded and actively feeding during the hours of darkness when, alone, zooplankton for their sustenance is abundant".

<sup>5</sup> Gladfelter (1982) also observed smaller fusiform crystals (ca. 1  $\mu\text{m}$  long) scattered on distal portions of the skeleton formed during the day. Constantz (1986a: 155) argued that a diurnal calcification pattern (i.e., daytime/fibrous and nighttime/equant) is predictable with the kinetic theory for control of crystal morphology, as lower nighttime temperatures reduce  $\text{CO}_2$  concentrations and thus change crystal growth kinetics and result in different crystal morphologies.

trices and, in turn, their influence on the composition and spatial arrangement on calcification styles (crystal shapes, etc.). However, existing data allow some speculation. Le Tissier (1988: 86) suggested that in *Pocillopora damicornis* two basic profiles of organic matrix (meshwork and sheets compartments, see Johnston 1980) fit perfectly the regions of separate formation of fusiform crystals and needle-shaped fasciculi, respectively (as noted above, fusiform crystals have been noticed only in night deposits in *Pocillopora*). On the other hand, Cuif and Sorauf (2001: 145) noted that the thickness of organic meshwork layer corresponds to that of (TD) fiber growth steps and perhaps this is composed of the soluble matrices whereas the organic envelopes (sheets compartments) that enclose bundles of fibers of insoluble components. Hence, one may speculate that, at least in some zooxanthellate corals, those regions enriched in organic components that repeatedly separate TD and dRAF fibrous layers correspond to the meshwork organic components, and fusiform crystals deposited during the night, whereas the needle-shaped crystals that form mineral TD and dRAF phases correspond to sheet compartments formed during the day. Further studies are required to confirm this hypothesis, especially on the composition and spatial arrangement of organic meshwork at the calcifying interface between crystals and calicoblastic cells localized specifically in dRAF and TD formation sites<sup>6</sup>.

In conclusion, there are several anatomical, physiological, and biochemical factors related to day-night cycles of the host and symbiotic partners that may cause distinct, night- and day micro- and nanoscale skeletal responses of zooxanthellate corals.

*Azooxanthellate corals.*—In comparison with zooxanthellate corals, organic-enriched phases in TD fibers of azooxanthellate corals are much less prominent and occur less regularly. On the other hand, prominent and surprisingly regular alternations of organo-mineral phases occur in the dRAF region of the same skeleton (e.g., Fig. 1E). What could be the cause of the general growth periodicity of azooxanthellate skeleton (1), and why is it much better expressed in RAF than TD regions (2)?

(1) In contrast to shallow-water settings of zooxanthellate corals, azooxanthellate corals examined herein<sup>7</sup> live in an aphotic environment with diurnal rhythms limited or not detectable. Mechanisms triggering microbanding in deep-water corals have been discussed, rather inconclusively, by Wells (1970), Sorauf and Jell (1977) and Lazier et al. (1999). However, Sorauf and Jell (1977: 16–18), in probably the most comprehensive discussion of the subject, suggested the

existence of some “biological clock [...] may be connected with enzyme production tied to a feeding cycle based on energy requirements of the coral polyps” as a plausible explanation of the tiny growth increments in *Desmophyllum cristagalli*. Because the several micrometer-scale skeletal increments of organo-mineral alternations in dRAF of azooxanthellate corals have a magnitude similar to the daily increments of zooxanthellate corals, it is tempting to suggest that they share a similar rhythm of diurnal formation (see also Sorauf and Jell 1977: 18). However, there is some evidence that supports and some that conflicts with this interpretation based on (a) estimations of the coral growth rates, and (b) in-vivo observations of the growing polyp.

(a) Information about growth of deep-water Scleractinia is very limited and concerns only a few species. Duncan (1877) estimated growth rates of *Lophelia* attached to the transatlantic cable at 6.8–7.5 mm/yr. Estimates of linear extension rate for the same species were 7.5–15 mm/yr by Teichert (1958), 6 mm/yr by Wilson (1979), and an average of 5.5 mm/yr by Mortensen and Rapp (1998). The latter authors implied that estimates by Freiwald et al. (1997), and Mikkelsen et al. (1982) of 25 mm/yr increments were erroneous, affected by sampling techniques. Cheng et al. (2000), using changes of <sup>230</sup>Th/<sup>232</sup>Th ratio with time in single septum of *D. cristagalli* (= *D. dianthus*), estimated an extension rate to be between 0.1 and 3.1 mm/yr. For the same species, Risk et al. (2002) suggest 0.5–1 mm/yr. Organo-mineral alternations of the smallest magnitude examined here in dRAF of *D. dianthus* have increments of ca. 2 μm; larger ones can be ca. 10 μm and more. Assuming that the smallest growth increments were formed during a diurnal cycle, that would translate to an annual linear extension rate of the septum of 0.73 mm. This estimate fits the yearly growth range estimated by Cheng, et al. (2000) and Risk et al. (2002).

(b) On the other hand, *in-vivo* observations of azooxanthellate corals by Roberts and Anderson (2002) indirectly suggest that estimates of skeletal growth based on minute-scale structures may be inaccurate. Using time-lapse video to record silhouettes of the polyps under infrared illumination, Roberts and Anderson (2002) showed that polyps of *Lophelia pertusa* behaved asynchronously and did not show any clear diurnal patterns over a three-day observation period. The authors speculate that periodic contraction and re-expansion of individual polyps may reflect a need to exchange water within the coelenteron or expel undigested food remains (noteworthy, expansion of zooxanthellate polyps may also be induced by factors other than light, e.g., high flow, and the presence of planktonic prey, though light re-

<sup>6</sup> Potentially, other factors may also cause organic- and mineral-phase alternations in skeleton. For example, in extremely shallow-water corals exposed to intertidal emersion, organic layers are apparently produced when calcium is unavailable (Dillon and Clark 1980; the same is known e.g., in barnacles, see Bourget 1987). However, TD organo-mineral alternation in zooxanthellate corals examined here are too dense and too regular to consider this as a putative cause.

<sup>7</sup> One specimen examined of the azooxanthellate “*Ceratotrochus*” *magnaghii* Cecchini, 1914 is from more shallow-water, a 50 m deep submarine cave. Although, the lack of illumination and generally oligotrophic conditions in deeper parts of submarine caves near Marseille resemble “stable” deep-water settings, seasonal water renewals (winter storms, spring water warming, etc.; for details see Fichez 1990) may influence coral growth according to shallow water rhythms.

mains the major trigger; Levy et al. 2001). Hence, if skeletal growth increments correlate with polyp's expansion-contraction cycles (as they might correlate in zooxanthellate corals, see Barnes 1972), then lack of distinct diurnal expansion behavior of azooxanthellate polyps (Roberts and Anderson 2002) may indicate other than daily amplitude of their minute-scale skeletal alternations.

Long-term research on physiology of, and biomineralization in, deep-water azooxanthellate corals may help assess actual timing of their skeletal growth increments. Another promising research direction to explain rhythmic changes in biomineralization are biogeochemical studies of components from successive organo-mineral bands (the effectiveness of such an approach was shown e.g., by Watabe et al. (1991) who demonstrated season-dependent and -independent organic components in spicules of the octocoral *Leptogorgia*).

(2) Marshall's (1996) studies on calcification of zooxanthellate and azooxanthellate corals shed some light on minute-scale skeletal differences between these corals as here described. Marshall (1996) argued that in azooxanthellate shallow-water *Tubastrea*, calcification is more balanced during night and day because it is not photosynthetically repressed, as in zooxanthellate corals. Hence, one would assume that similar "balanced" calcification occurs in other azooxanthellate corals, especially those living in the deep-water aphotic zone where diurnal differences influencing calcification are limited or absent.

This may also explain the lack of prominent organic-enriched layers in TD fibers of azooxanthellate corals versus the prominent development of them in zooxanthellate corals. As speculated above (p. 519), enhanced growth may be attained by increased formation of organic rather than mineral phases, hence dRAF regions in azooxanthellate corals may also have prominent organic-enriched phases due to their faster growth.

## Remarks on taphonomy of dRAF and TD deposits

Origin of several types of diagenetic structures of dRAF and TD can best be understood given its original organo-mineral composition (the influence of organic components on skeletal diagenesis was recently discussed by Sorauf and Cuif 2001). The following aspects of diagenesis are commented on here: (1) vestiges of dRAF in recrystallized coralla, and (2) alternations of optically darker and lighter TD layers in fossil corals with their original aragonitic mineralogy preserved.

(1) Occasionally, in completely recrystallized coralla, regularly distributed dark brown spots or distinctly lighter regions can be observed along the mid-septal zone and in centers of septal granulations. The position of these structures suggests a relation to the dRAF and their regular distribution implies formation before recrystallization of the skeleton (they were described as vestiges of "centers of calcification" by Morycowa and Roniewicz 1990, Stolarski 1990). Com-

monly, dark-brown or light color of these structures results from enrichment in Fe-Mn (Freiwald and Wilson 1998; Sorauf and Freiwald 2002), or, respectively in Si minerals (e.g., Gautret et al. 2000). In modern corals, diagenetic Fe-Mn minerals are deposited in dRAF regions enriched in organic components that are nourishment for endolithic fungi associated with iron-manganese precipitating bacteria (Freiwald and Wilson 1998). Such preferential bioerosion of dRAF regions ("centers of calcification") enriched in organic matter was observed in modern scleractinian coralla (Cuif and Dauphin 1998: figs. 1.7, 1.8). Decomposition of organic components may lead to local lowering of pH and, in environments rich in silica, precipitation of this mineral. Because biochemical composition and properties of skeletal organic materials differ between taxa (e.g., Cuif et al. 1997) this may result in different diagenetic patterns that, *vice versa*, can serve as a taxonomic proxy in fossil corals. Such an interpretation requires particular caution, as other skeletal properties and environmental factors may result in differential diagenesis.

(2) The TD fibers of all modern corals show periodic alternations of organic-enriched and mineral phases (particularly regular and distinct in zooxanthellate taxa). A lack of "repartition of organic compounds within crystal-like fibers" in aragonitic corallum of *Pachytheccalis major* Cuif, 1975 (Triassic, Alakir Çay, Turkey) led Cuif, Dauphin and Gautret (1999: 590) to conclude that an "additional mineral component has been added during fossilization process, possibly as syntaxial deposit". Intriguingly, coralla of *P. major* and *Pachysolenia cylindrica* Cuif, 1975 from the same Turkish locality examined here show fine alternations of darker and lighter regions (in TLM), and occasional regular differences in etching relief of wall fibers. Optical alternations occur every 5–8  $\mu\text{m}$  that corresponds roughly to microbandings in modern corals. An indication that at least organic-enriched components of the pachytheccaliinan coralla underwent diagenetic changes is the lack of a distinct fluorescence response of the coralla stained with acridine orange dye. This is in agreement with Cuif et al. (1992) and Gautret and Marin (1993) analyses that only a small fraction of the organic components typical of modern coralla is preserved in fossils (e.g., even Eocene scleractinians with aragonitic skeleton retained only 1–7% amount of organic components of extant corals). If diagenesis only affects regions originally enriched in organic matter, as suggested by Cuif, Dauphin and Gautret (1999), one would expect an alternation of fine diagenetically altered and unaltered zones. However, such a clear-cut pattern has not been observed in elemental X-ray mapping of microbanded skeletal parts. The distribution pattern of Sr and Mg (common trace element in calcite) is generally irregular, although some more longitudinal (along fibers) and transverse (across fibers) linear grouping of pixels are also visible. Regions enriched in Sr appear depleted in respect to Mg and *vice versa*. This suggests some diagenetic change (?calcitization) of the originally aragonitic skeleton that, however, were not limited to the dark (or transparent)

zones of the skeleton (Fig. 14A–C<sup>8</sup>). Also, the etching relief of the TD fibers of pachythea in *P. cylindrica* and *P. major*, has a “carved” and slightly irregular appearance in comparison to the sharp and distinct “fissures” or tapering of fibers between etched layers of fibers in modern and also Triassic corals (including the pachythealiid *Z. zardini*) from Alpe di Specie in Italy (Figs. 3A, 5B, 7A, 12C, 15C).

The above evidence suggests that: a) organo-mineral discontinuities typical of diagenetically unaffected coralla are faded in the Triassic pachythealiinans from Alakir Çay (assuming, their original occurrence) and b) that overall “excellently preserved” fibrous skeleton shows diagenetic alternation at the scale of “individual fibers”. Alternations of darker and lighter zones in fibrous wall may represent diagenetic ghost structures whose origin and regular distribution was controlled by the spatial configuration and biochemical composition of original intracrystalline organic matrices. Additional high-resolution geochemical studies (currently underway) are necessary to support this hypothesis.

### Phylogenetic significance of minute-scale structures

Phylogenetic hypotheses based on molecular data very often differ significantly from those constructed on macro- or microstructural skeletal characters gathered in conventional ways (e.g., Veron et al. 1996; Romano and Cairns 2000). Caryophyllinans (the suborder that includes all azooxanthellate taxa examined here) provide a good example of acoral group in which molecular and traditional phylogenetic hypotheses are conflicting. Traditionally, monophyly of the group is based on their smooth septal margin (Vaughan and Wells 1943), or according to microstructural criteria, on a narrow mid-septal zone composed of “minitrabeculae” (traditional Caryophyllina are a synonym of “minitrabecular” corals of Roniewicz 1989). Conversely, molecular data strongly support paraphyly of caryophyllinans since their various groups are dispersed along the tree topology (Romano and Cairns 2000; Cuif et al. 2003). For example, on Romano and Cairns’ (2000) 16S and 28S rDNA trees topology, it is striking that there is wide separation of clades that include *Caryophyllia* and *Flabellum*. However, Cuif et al. (2003) showed that phylogenetic hypotheses based on more in-depth microstructural analysis may corroborate molecular ones, e.g., molecular studies support polyphyly of the traditional Guyniidae, an hypothesis put forward for the first time on the basis of very different distribution of septal and wall “centers of calcification” in traditional guyniid taxa (hypothesis “A” by Stolarski 2000). Additional characters disclosed in corallum analysis proposed here may help further in the “fine-tuning” phylogenetic hypotheses concerning this and other coral groups. Preliminary observations suggest, for example, that *Flabellum*, in contrast to *Stephanocyathus*, or “*Ceratotrochus*”, has CRA that are small and well separated

from each other, and unique scale-like organization of TD fibers (this feature also occurs in many species of *Flabellum*, some other flabellid genera, and can be compared with various species of *Stephanocyathus* and similar caryophylliid genera). On the other hand, “*Ceratotrochus*” *magnaghii* forms a distinct clade with *Vaughanella* and *Odontocyathus* (Romano and Cairns 2000) on molecular tree topology, in contrast to other caryophyllinans examined here, and seemingly has a homogenous structure of dRAF, actually composed of very narrow “strands”.

Recent studies of stylophyllinans provide examples of fossil corals whose more in-depth skeletal analysis recognized inconsistencies in traditional microstructural approaches. Traditionally, they are considered “non-trabecular” corals (Beauvais 1982; Roniewicz 1989). The antonymy between “non-trabecular” (Stylophyllina) and “trabecular” (all other scleractinian groups) implies a fundamental difference between these corals (noteworthy, Cuif (1977) described stylophyllid septa built of “trabecula-like” elements; also Roniewicz (1989) described an “axial rod or plate” in some stylophyllid septa that clearly refers to “mid-septal” zone of “trabecular” corals). However, diverse microstructural patterns observed in transverse sections of various stylophyllids (including forms with minute and large “centers of calcification”) showed that distinction between “trabecular” *versus* “non-trabecular” corals is unclear, at least concerning stylophyllinans with “centers of calcification” (Stolarski and Russo 2002). This study confirms the “typical” nature of large “centers of calcification” as appears in longitudinal sections of septal spines of *Stylophyllum paradoxum*, just as in “trabecular corals”: fibrous layers that are regularly separated by zones infilled by sparite (originally, most likely, composed of organic enriched components). In comparison with modern “trabecular corals” examined here, fibrous layers of *S. paradoxum* are more widely spaced (every ca. 30–40  $\mu\text{m}$  *versus* few micrometers in modern “trabecular” corals). The lack of a narrow 10–20  $\mu\text{m}$  “border layer between centers and fibers” noticed by Stolarski and Russo (2002: 662) also seems to result from much thicker fibrous envelopes of the dRAF zone (Fig. 13D, E). On the other hand, irregular, occasionally >20  $\mu\text{m}$  thick dRAF fibrous layers occur in the dRAF of the Triassic conophylliid noted earlier, suggesting that more observations are needed to verify the possible taxonomic value of this character.

### Conclusions

- The entire septal skeleton of corals is composed of alterations of mineral and organic-enriched phases. They form superimposed layers that may be interrupted in some directions of growth but in other directions there is continuity between “centers of calcification” and “fibers”, making distinction between these two structures unclear. The “lay-

<sup>8</sup> It is noteworthy that changes in the skeletal Sr-Ca ratio can also originally be caused by temperature-related factors (e.g., Allison et al. 2001).

ered model” of skeletal growth proposed as an alternative to the traditional “two-step model” explains the differences between “centers of calcification” and “fibers” in terms of differential growth dynamics (and not necessarily different timing) between these regions. Instead of the inadequate “trabecular concept” and “centers of calcification”, a distinction between deposits of the Rapid Accretion Front (dRAF; which in particular cases can be organized into Centers of Rapid Accretion, CRA) and Thickening Deposits (TD) is proposed.

- dRAF are built of regular alternations of mineral and organic phases: successive thin layers of mineral phase that enclose organic lens-shaped layers are composed of short (1.5–5  $\mu\text{m}$  in length) but not isometric (as commonly assumed) aragonite fibers. Nanometer-scale (ca. 50 nm in diameter) mineral components shown in dRAF seem to match the size range of nodular structures interpreted recently by Clode and Marshall (2003b) as nascent  $\text{CaCO}_3$  crystals developed upon a fibrillar organic matrix in the sub-epithelial space.
- The remarkable regularity of mineral/organic phase alterations in TD skeleton of zooxanthellate corals and lack of such regularity in azooxanthellate coralla appears to be a promising criterion to distinguish these two ecologically distinct coral groups on the skeletal basis, possible also in fossils. This may supplement Cuif et al. (1999) finding that it is possible to discriminate between symbiotic or non-symbiotic coral metabolism through the biochemical compositions of their mineralizing matrices.
- The dRAF in some “non-trabecular” stylophyllids appear to differ only quantitatively from typical “trabecular” scleractinians. Taxonomic revision and reassessment of phylogenetic position of this, and other groups of corals, is pending.

## Glossary

This glossary provides a quick guide to traditionally used and newly proposed microstructural terminology.

**Centers of Rapid Accretion (CRA, new term)**—well differentiated regions of skeletal rapid accretion. Alternations of organo-mineral deposits formed in this region (**deposits of Centers of Rapid Accretion, dCRA, new term**) differ from the adjacent  $\rightarrow$  Thickening Deposits, in significantly higher amount of organic components. CRA may be closely spaced on a distal septal margin or on a more or less continuous zone (variety of  $\rightarrow$  Rapid Accretion Front), or be widely separated from each other. The latter results in formation of denticulations (teeth) on the distal septal margin or, if CRA occur on septal flanks, in the development of granulations. Traditionally, CRA have been recognized in transverse sections of septa and in certain types of corallite wall (marginotheca, trabeculotheca, see Stolarski 1995) as  $\rightarrow$  centers of calcification.

**Centers of calcification**—structures traditionally recognized in transverse sections of various skeletal elements as “dark spots [...] from which fascicles of fibrous crystals radiate toward those of neighboring centers” (Vaughan and Wells 1943: 32). They were considered “circular in section, sometimes [...] elliptical” (Ogilvie 1897: 113)

## Acknowledgements

Particular thanks should go to my colleagues Steve Cairns (Smithsonian Institution, Washington, D.C.), Jean-Pierre Cuif (Université Paris XI Orsay), Antonio Russo (Università di Modena e Reggio Emilia, Italy), and Helmut Zibrowius (Station Marine d’Endoume, Marseille) who generously provided specimens of Recent (S.C., H.Z.) and Triassic (J.-P.C., A.R.) corals for this study. I was always able to count on the help and advice of my colleague and friend Ewa Roniewicz, and especially so concerning Triassic corals. The role of *accoucheurs* for some ideas presented in this paper was played by the following friends (even those who are not specialists on coral biomineralization), who devoted their time for discussions and enthusiastic support during the most painful periods of this work: Steve Cairns (Smithsonian Institution), Tomasz Baumiller (University of Michigan, USA); Tomasz Grycuk (Institute of Experimental Physics, Warsaw University), and Maciej Mazur (Faculty of Chemistry, Warsaw University; Maciej also helped in making AFM observations on coral samples). S. Cairns and T. Baumiller also corrected the language of some chapters of this manuscript. Skills and knowledge concerning MFM techniques were generously shared with me by Władysław Cabaj and Elżbieta Kędra (both from the Institute of Parasitology, Warsaw), Michał Wojciechowski and Tomasz Ziółkowski (both from Precoptic Co.-Nikon, Warsaw). Excellent thin sections were prepared by Zbigniew Strąk (ZPAL), and Bogusław Waksmundzki (Faculty of Geology, Warsaw University) brilliantly rendered the objects in the composition of Fig. 17. Critically constructive comments of the reviewers of this paper (Jim Sorauf, Binghamton University, USA, and an anonymous reviewer) were appreciatively received and treasured. Jim Sorauf aided in anglicizing my Polish English. Without the aid of all of the above individuals this work would have been impossible. I would like also to express my gratitude for the sponsorship given by the Smithsonian Institution (short-term scholarship in March 2003), Italian Ministry of University and Scientific and Technological Research Grant MURST (project Cofin 2002), and State Committee for Scientific Research (KBN) grant 6 P04D 007 23 to J. Stolarski.

in shape, “marking the central point from which calcification has taken place” (Bourne 1887: 41; see also Fowler 1887: 7). According to some authors they were considered entirely mineral (i.e., “crystals [...] less than 1  $\mu\text{m}$  in diameter and [...] randomly oriented” Wainwright 1964). More recently, they were considered as forming a homogenous structure built of “tiny crystals (size 1 micron), densely packed, rather randomly oriented, and [...] embedded in an organic component” (Cuif and Dauphin 1998). “Centers of calcification” are synonymous with  $\rightarrow$  trabecular (or  $\rightarrow$  sclerodermite) axes. In this work they are redefined as deposits of Centers of Rapid Accretion ( $\rightarrow$  Centers of Rapid Accretion)

**Rapid Accretion Front (RAF, new term)**—more or less continuous zone of rapid skeletal accretion (e.g., crest of septum, pali, paliform lobe, wall, columella). Regularly alternating organo-mineral deposits formed in this region (**deposits of Rapid Accretion Front, dRAF, new term**) differ from the adjacent  $\rightarrow$  Thickening Deposits, in their significantly higher content of organic components. Organo-mineral layers may continue or be interrupted between dRAF and TD regions. Depending on analytical means and interpretations, dRAF have been formerly described as: “dark line”, primary streak, primary septum, Uhrseptum, or by the neutral term

mid-septal zone in which often individual and densely packed → centers of calcification were recognized (see review in Ogilvie 1897). Recently, Cuif, Dauphin et al. (2003) coined a new term Early Mineralization Zone (EMZ) as “trace of the distal growth edge within the septum” (Cuif et al. 2003 used modified version of this term Early Calcification Zone, ECZ). However, continuity between dRAF and → TD (at least in some directions of growth) supports the idea adopted in this paper that differences between these two regions results from differential growth dynamics (not necessarily different timing).

**Sclerodermite**—term introduced by Milne Edwards and Haime (1857: 32) to describe nodular structures (“sclerites”) whose linear series unite to form “poutrelles” (synonym of → trabeculae). Sclerodermites were later reinterpreted as basic units of the coral skeleton composed of → centers of calcification together with their clusters of fibers that when arranged vertically produce a trabecula (Vaughan and Wells 1956; Barnes 1970, see also geometrical visualization of sclerodermite segments by Alloiteau 1957: 19, 35). The idea of sclerodermite was abandoned e.g., by Gill (1967) who considered trabeculae as continuously growing rods not divided into any modules. In this paper I demonstrated that structures formerly called trabeculae (dRAF, dCRA) are actually composed of regular alternations of organo-mineral phases and hence do not form continuously growing rods (in terms of continuous deposition of homogenous components). However, sclerodermite is not applicable to any of these mineral or organic components since they do not form structurally limited regions.

**Trabeculae** (Trabekeln of Pratz 1882, poutrelles of Milne Edwards and Haime 1857)—traditionally defined as pillars or rods (divided or not into → sclerodermites) of calcareous fibers radiating from → centers of calcification that are aligned in axes (Vaughan and Wells 1943). According to Bryan and Hill (1942: 79) model of spherulitic growth, trabeculae represent “axiolitic type” spherulites, each be-

ing “a cylinder tapering convexly at the top, and consisting of fibres, usually curved, directed upwards and outwards from a common axis”. Trabeculae recognized in transverse or longitudinal-radial sections of septa were categorized in different size classes (minitrabeculae or thick trabeculae of Roniewicz 1989) that served as subordinal taxonomic criteria. Difficulties where to set the boundary between trabeculae and fibrous tissue (→ Thickening Deposits) were side-stepped by interpolating their dimensions by measuring distances between neighboring centers of calcification. Sections perpendicular to the septal plane clearly showed that organo-mineral layers may continue between regions formerly called trabecular axes (→ centers of calcification) and fibers (stereome) making trabecular concept vague and not applicable in model of skeletal growth presented in this paper.

**Thickening Deposits (TD, new term)**—skeletal structures deposited outside the areas of rapid skeletal accretion (i.e., Rapid Accretion Front, Centers of Rapid Accretion), although organo-mineral components may form continuous layers from one to the other. TD differs from dRAF/dCRA in having significantly lesser amounts of the organic component in its organo-mineral alternations. In zooxanthellate corals, TD seem to form very regular organo-mineral alternations with slightly thicker organic phases whereas organo-mineral alternations of TD in azooxanthellate corals appear to be less regular. There are several formal or informal terms that have been previously used to describe fibrous deposits “not organized in trabeculae”, e.g., stereoplasm, secondary thickening (see Ogilvie 1897), stereome (see Vaughan and Wells 1943; Sorauf 1972), or tectura (Stolarski 1995). In the proposed layered model of skeletal growth the main distinction between skeletal deposits is whether they are formed in regions of rapid accretion (RAF, CRA) or in regions of less active skeletal deposition. In expressing this simple distinction I prefer to avoid using any older terms having various connotations, hence am proposing the new term, TD.

## References

- Alcock, A. 1902. Diagnoses and descriptions of new species of corals from the Siboga expedition. *Tijdschrift der Nederlandsche Dierkundige Vereeniging* 7: 89–115.
- Al-Horani, F.A., Al-Moghrabi, S.M., and De Beer, D. 2003. The mechanism of calcification and its relation to photosynthesis and respiration in the scleractinian coral *Galaxea fascicularis*. *Marine Biology* 142: 419–426.
- Allemand, D., Tambutté, É., Girard, J.-P., and Jaubert, J. 1998. Organic matrix synthesis in the Scleractinian coral, *Stylophora pistillata*: role in biomineralization and potential target of the organotin TBT. *Journal of Experimental Biology* 201: 2001–2009.
- Allison, N., Finch, A., Sutton, S., and Newville, M. 2001. Strontium heterogeneity and speciation in coral aragonite; implications for the strontium paleothermometer. *Geochimica et Cosmochimica Acta* 65: 2669–2676.
- Alloiteau, J. 1957. Contribution a la systématique des Madréporaires fossiles. *Centre Nationale de la Recherche Scientifique* 1: 1–426.
- Barnes, D.J. 1970. Coral skeleton: an explanation of their growth and structure. *Science* 170: 1305–1308.
- Barnes, D.J. 1972. The structure and formation of growth-ridges in scleractinian coral skeletons. *Proceedings of the Royal Society of London B* 182: 331–350.
- Barnes, D.J. and Chalker, B.E. 1990. Calcification and photosynthesis in reef-building corals and algae. In: Z. Dubinsky (ed.), *Coral Reefs* (Ecosystems of the world 25), 109–131. Elsevier, Amsterdam.
- Barnes, D.J. and Crossland, C.J. 1980. Diurnal and seasonal variations in the growth of a staghorn coral measured by time-lapse photography. *Limnology and Oceanography* 25: 1113–1117.
- Beauvais, L. 1982. Sur la taxonomie des Madréporaires mésozoïques. *Acta Palaeontologica Polonica* 25: 345–360.
- Bourne, G.C. 1887. On the anatomy of *Mussa* and *Euphyllia*, and the morphology of the madreporarian skeleton. *Quarterly Journal of Microscopical Science* 28: 21–52.
- Bryan, W.H. and Hill, D. 1942. Spherulitic crystallization as a mechanism of skeletal growth in the hexacorals. *Proceedings of the Royal Society of Queensland* 52: 78–91.
- Cairns, S.D. 1977. A revision of the recent species of *Stephanocyathus* (Anthozoa: Scleractinia) in the western Atlantic, with descriptions of two new species. *Bulletin of Marine Science* 27: 729–739.
- Cairns, S.D. 1979. The deep-water Scleractinia of the Caribbean Sea and adjacent waters. *Studies on the fauna of Curaçao and other Caribbean islands* 67 (180): 341.
- Cairns, S.D. 1995. The marine fauna of New Zealand: Scleractinia (Cnidaria: Anthozoa). *New Zealand Oceanographic Institute Memoir* 103: 1–210.
- Cecchini, C. 1914. Su due nuovi Turbinolidae del Mediterraneo (diagnosi preliminari). *Monitore Zoologico Italiano* 25: 151–152.
- Cheng, H., Adkins, J.F., Edwards, R.L., and Boyle, E.A. 2000. 230Th dating of deep-sea corals. *Geochimica et Cosmochimica Acta* 64: 2401–2416.
- Clode, P.T. and Marshall, A.T. 2002. Low temperature FESEM of the calcifying interface of a scleractinian coral. *Tissue and Cell* 34: 187–198.
- Clode, P.T. and Marshall, A.T. 2003a. Skeletal microstructure of *Galaxea fascicularis* exsert septa: a high-resolution SEM Study. *Biological Bulletin* 204: 146–154.

- Clode, P.T. and Marshall, A.T. 2003b. Calcium associated with fibrillar organic matrix in the scleractinian coral *Galaxea fascicularis*. *Protoplasma* 220: 153–161.
- Constantz, B.R. 1986a. Coral skeleton construction: a physiochemically dominated process. *Palaios* 1: 152–157.
- Constantz, B.R. 1986b. The primary surface area of corals and variations in their susceptibility to diagenesis. In: J.H. Schroeder and B.H. Purser (eds.), *Reef Diagenesis*, 77–90. Springer Verlag, Berlin.
- Constantz, B.R. and Meike, A. 1990. Calcite centers of calcification in *Mussa angulosa* (Scleractinia). In: R.E. Crick (ed.), *Origin, Evolution, and Modern Aspects of Biomineralization in Plants and Animals*, 201–207. Plenum Press, New York.
- Cuif, J.P. 1973. Recherches sur les Madréporaires du Trias. I. Famille Stylophyllidae. *Bulletin du Muséum National d'Histoire naturelle, sér. 3, 97, Sciences de la Terre* 17: 211–291.
- Cuif, J.P. 1975. Caractères morphologiques, microstructuraux et systématiques des Pachytheclidae, nouvelle famille de Madréporaires triasiques. *Geobios* 8: 157–180.
- Cuif, J.P. 1977. Arguments pour une relation phylétique entre les madréporaires paléozoïques et ceux du Trias. Implications systématiques de l'analyse microstructurale des Madréporaires triasiques. *Mémoires de la Société Géologique de France* 129: 1–54.
- Cuif, J.P. and Dauphin, Y. 1998. Microstructural and physico-chemical characterization of “centers of calcification” in septa of some Recent scleractinian corals. *Paläontologische Zeitschrift* 72: 257–270.
- Cuif, J.P. and Sorauf, J.E. 2001. Biomineralization and diagenesis in Scleractinia: part I, biomineralization. *Bulletin of the Tohoku University Museum* 1: 144–151.
- Cuif, J.P., Dauphin, Y., and Gautret, P. 1997. Biomineralization features in scleractinian coral skeletons: source of new taxonomic criteria. *Boletín de la Real Sociedad Española de Historia Natural (Sección Geológica)* 92: 129–141.
- Cuif, J.P., Dauphin, Y., and Gautret, P. 1999. Compositional diversity of soluble mineralizing matrices in some recent coral skeletons compared to fine-scale growth structures of fibers: discussion of consequences for biomineralization and diagenesis. *International Journal of Earth Sciences* 88: 582–592.
- Cuif J.P., Dauphin, Y., Denis A., Gautret, P., Lawniczak, A., and Raguideau, A. 1987. Résultats récents concernant l'analyse des biocristaux carbonatés; implications biologiques et sédimentologiques. *Bulletin de la Société Géologique de France 8e ser., III, 2*: 269–288.
- Cuif, J.P., Dauphin, Y., Doucet, J., Salome, M., and Susini, J. 2003. XANES mapping of organic sulfate in three scleractinian coral skeleton. *Geochimica et Cosmochimica Acta* 67: 75–83.
- Cuif, J.P., Dauphin, Y., Freiwald, A., Gautret, P., and Zibrowius, H. 1999. Biochemical markers of zooxanthellae symbiosis in soluble matrices of skeleton of 24 Scleractinia species. *Comparative Biochemistry and Physiology A* 123: 269–278.
- Cuif, J.P., Denis, A., Gautret, P., Marin, F., Mastandrea, A., and Russo, F. 1992. Recherches sur l'altération diagénétique des biominéralisations carbonatées: évolution de la phase organique intrasquelettique dans des polypiers aragonitiques de Madréporaires du Cénozoïque (Bassin de Paris) et du Trias supérieur (Dolomites et Turquie). *Comptes Rendus de l'Académie des Sciences de Paris* 314: 1097–1102.
- Cuif, J.P., Lecoindre, G., Perrin, C., Tillier, A., and Tillier, S. 2003. Patterns of septal biomineralization in Scleractinia compared with their 28S rRNA phylogeny: a dual approach for a new taxonomic framework. *Zoologica Scripta* 32: 459–473.
- Dauphin, Y. 2001. Nanostructures de la nacre des tests de céphalopodes actuels (Nanostructures of the nacreous layers in Recent cephalopod shells). *Paläontologische Zeitschrift* 75: 113–122.
- De Beer, D., Kühl, M., Stambler, N., and Vaki, L. 2000. A microsensor study of light enhanced Ca<sup>2+</sup> uptake and photosynthesis in the reef-building hermatypic coral *Favia* sp. *Marine Ecology Progress Series* 194: 75–85.
- Dillon, J.F. and Clark, G.R. II. 1980. Growth line analysis as a test for contemporaneity in populations. In: D.C. Rhoads and R.A. Lutz (eds.), *Skeletal Growth in Aquatic Organisms*, 395–415. Plenum, New York.
- Domart-Coulon, I.J., Elbert, D.C., Scully, E.P., Calimlim, P.S., and Ostrander, G.K. 2001. Aragonite crystallization in primary cell cultures of multicellular isolates from a hard coral, *Pocillopora damicornis*. *Proceedings of the National Academy of Sciences* 98: 11885–11890.
- Duerden, J.E. 1902. West Indian madreporarian polyps. *National Academy of Sciences (Washington), Memoir* 7: 399–648.
- Duncan, P.M. 1876. Notices of some deep-sea and littoral corals from the Atlantic Ocean, Caribbean, Indian, New-Zealand, Persian Gulf, and Japanese & c. Seas. *Proceedings of the Zoological society of London* 1876: 428–442.
- Duncan, P.M. 1877. On the rapidity of growth and variability of some Madreporaria on an Atlantic cable, with remarks upon the rate of accumulation of Foraminiferal deposits. *Proceedings of the Royal Society of London* 26 (180): 133–137.
- Ellis, J. and Solander, D. 1786. *The Natural History of Many Curious and Uncommon Zoophytes, Collected From Various Parts of the Globe*. xii + 206 pp. B. White and son, P. Elmsly, London.
- Esper, E.J.C. 1794. *Fortsetzungen der Pflanzenthier in Abbildungen nach der Natur mit Farben erleuchtet*. Vol. 1 (1–2). 64 pp. Nürnberg.
- Fedorowski, J. 1974. The Upper Palaeozoic tetracoral genera *Lophophyllum* and *Timorphyllum*. *Palaeontology* 17: 441–473.
- Fichez, R. 1990. Decrease in allochthonous organic inputs in dark submarine caves, connection with lowering in benthic community richness. *Hydrobiologia* 207: 61–69.
- Fowler, G.H. 1887. The anatomy of the Madreporaria. III. *Quarterly Journal of Microscopical Science* 28: 1–19.
- Frech, F. 1890. Die Korallenfauna der Trias. Die Korallen der juvavischen Triasprovinz. *Palaeontographica* 37: 1–116.
- Freiwald, A. and Wilson, J.B. 1998. Taphonomy of modern deep, cold-temperate coral reefs. *Historical Biology* 13: 37–52.
- Freiwald, A., Henrich, R., and Pätzold, J. 1997. Anatomy of a deep-water coral reef mound from Stjernsund, West Fimmark, North Norway. *Society for Sedimentary Geology, Special Volume* 56: 141–162.
- Fukuda, I., Ooki, S., Fujita, T., Murayama, E., Nagasawa, H., Isa, Y., and Watanabe, T. 2003. Molecular cloning of a cDNA encoding a soluble protein in the coral exoskeleton. *Biochemical and Biophysical Research Communications* 304: 11–17.
- Gautret, P. and Marin, F. 1993. Evaluation of diagenesis in scleractinian corals and calcified demosponges by substitution index measurement and intraskeletal organic matrix analysis. *Courier Forschungsinstitut Senckenberg* 164: 317–327.
- Gautret, P., Cuif, J.P., and Stolarski, J. 2000. Organic components of the skeleton of scleractinian corals—evidence from *in situ* acridine orange staining. *Acta Palaeontologica Polonica* 45: 107–118.
- Gill, G.A. and Lafuste, J.G. 1971. Madréporaires simples du Dogger d'Afghanistan: étude sur les structures de type “*Montlivaltia*”. *Mémoires de la Société Géologique de France (n.s.)* 50: 1–40.
- Gladfelter, E.H. 1982. Skeletal development in *Acropora cervicornis*: I. Patterns of calcium carbonate accretion in the axial corallite. *Coral Reefs* 1: 45–51.
- Gladfelter, E.H. 1983. Skeletal development in *Acropora cervicornis* II. Diel patterns of calcium carbonate accretion. *Coral Reefs* 2: 91–100.
- Goreau, T.F. 1959. The physiology of the skeleton formation in corals. I. A method for measuring the rate of calcium deposition by corals under different conditions. *Biological Bulletin* 116: 59–75.
- Goreau, N.I. and Hayes, R.L. 1977. Nucleation catalysis in coral skeletogenesis. *Proceedings, Third International Coral Reef Symposium, Rosenstiel School of Marine and Atmospheric Science, Miami* 2 (Geology), 439–445.
- Goldberg, W.M. 2001. Acid polysaccharides in the skeletal matrix and calicoblastic epithelium of the stony coral *Mycetophyllia reesi*. *Tissue and Cell* 33: 376–387.
- Gravier, C.J. 1915. Sur quelques traits de la biologie des Coraux des grandes

- profondeurs sousmarines. *Comptes rendus hebdomadaires des séances de l'Académie des sciences* 160 (12): 380–382.
- Grégoire, C. 1987. Ultrastructure of the *Nautilus* shell. In: W.B. Saunders and N.H. Landman (eds.), *Nautilus: The Biology and Paleobiology of a Living Fossil*, 463–486. Plenum Press, New York.
- Hayes, R.L. and Goreau, N.I. 1977a. Cytodynamics of coral calcification. *Proceedings, Third International Coral Reef Symposium, Rosenstiel School of Marine and Atmospheric Science, Miami*, 433–438.
- Hayes, R.L. and Goreau, N.I. 1977b. Intracellular crystal-bearing vesicles in the epidermis of scleractinian corals, *Astrangia danae* (Agassiz) and *Porites porites* (Pallas). *Biological Bulletin* 152: 26–40.
- Hidaka, M. 1991a. Deposition of fusiform crystals without apparent diurnal rhythm at the growing edge of septa of the coral *Galaxea fascicularis*. *Coral Reefs* 10: 41–45.
- Hidaka, M. 1991b. Fusiform and needle-shaped crystals found on the skeleton of a coral, *Galaxea fascicularis*. In: S. Suga and H. Nakahara (eds.), *Mechanisms and Phylogeny of Mineralization in Biological Systems*, 139–143. Springer Verlag, Tokyo.
- Howe, S.A. and Marshall, A.T. 2002. Temperature effects on calcification rate and skeletal deposition in the temperate coral, *Plesiastrea versipora* (Lamarck). *Journal of Experimental Marine Biology and Ecology* 275: 63–81.
- Ijina, T.G. [Il'ina, T.G.] 1984. Historical development of corals [in Russian]. *Trudy Paleontologičeskogo Instituta* 198: 1–183.
- Isa, Y. 1986. An electron microscope study on the mineralization of the skeleton of the staghorn coral *Acropora hebes*. *Marine Biology* 93: 91–101.
- Jell, J.S. 1974. The microstructure of some scleractinian corals. *Proceedings of the 2nd International Coral Reef Symposium, Brisbane* 2: 301–320.
- Jell, J.S. 1975. Preliminary notes on the microstructure and growth of scleractinian corals. *Proceedings of Crown-of-Thorns Starfish Seminar, Brisbane, 6th September 1974*. Australian Government Publishing Service, Canberra.
- Jell, J.S. and Hill, D. 1974. The microstructure of corals. In: B.S. Sokolov (ed.), *Ancient Cnidaria (Vol. 1)*, 8–14. Nauka, Novosibirsk.
- Johnston, I.S. 1980. The ultrastructure of skeletogenesis in hermatypic corals. *International Review of Cytology* 67: 171–214.
- Kato, M. 1963. Fine skeletal structures in Rugosa. *Journal of the Faculty of Science Hokkaido University* 11: 571–630.
- Koch, G., von. 1882. Über die Entwicklung des Kalkskeletes von *Asteroides calycularis* und dessen morphologische Bedeutung. *Mittheilungen aus der Zoologischen Station zu Neapel* 3: 284–292.
- Koker, E.M.J. 1924. Anthozoa uit het Perm van het eiland Timor, I: Zaphrentidae, Plerophyllidae, Cystiphyllidae, Amphiastreaeidae. *Jaarboek van het mijnwezen in Nederlandsch Oost-Indië* 51 (1922): 1–50.
- Lazier, A.V., Smith, J.E., Risk, M.J., and Schwarcz, H.P. 1999. The skeletal structure of *Desmophyllum cristagalli*: the use of deep-water corals in sclerochronology. *Leithaia* 32: 119–130.
- Le Tissier, M.d'A. 1988. Patterns of formation and the ultrastructure of the larval skeleton of *Pocillopora damicornis*. *Marine Biology* 98: 493–501.
- Le Tissier, M.d'A. 1991. The nature of the skeleton and skeletogenic tissue in the Cnidaria. *Hydrobiologia* 216/217: 397–402.
- Levy, O., Mizrahi, L., Chadwick-Furman, N.E., and Achituv, Y. 2001. Factors controlling the expansion behavior of *Favia favaus* (Cnidaria: Scleractinia): Effects of light, flow, and planktonic prey. *Biological Bulletin* 200: 118–126.
- Linnaeus, C. 1767. *Systema naturae, sive Regna tria Naturae systematice proposita per classes, ordines, genera et species* 1 (2) 12 edition, 533–1327. Laurentius Salvius, Stockholm.
- Marenzeller E., von. 1904. Steinkorallen. *Wissenschaftliche Ergebnisse der Deutschen Tiefsee-Expedition auf dem Dampfer "Valdivia" 1898–1899*, 7 (3): 261–318.
- Marenzeller, E., von 1888. Ueber einige japanische Turbinoliiden. *Annales des K.-K. Naturhistorischen Hofmuseums Wien* 3: 15–22.
- Marshall, A.T. 1996. Calcification in hermatypic and ahermatypic corals. *Science* 271: 637–639.
- Marshall, A.T. and Clode, P. 2002. Effect of increased calcium concentration in sea water on calcification and photosynthesis in the scleractinian coral *Galaxea fascicularis*. *The Journal of Experimental Biology* 205: 2107–2113.
- Marshall, A.T. and Wright, A. 1998. Coral calcification: autoradiography of a scleractinian coral *Galaxea fascicularis* after incubation in <sup>45</sup>Ca and <sup>14</sup>C. *Coral Reefs* 17: 37–47.
- Matthai, G. 1914. A revision of the Recent colonial *Astraeidae* possessing distinct corallites. *Transactions of the Linnean Society of London, Ser. 2 (Zoology)* 17: 1–140.
- McConnaughey, T.A. 1989. Biomineralization mechanisms. In: R.E. Crick (ed.), *Origin, Evolution, and Modern Aspects of Biomineralization in Plants and Animals*, 57–73. Plenum Press, New York.
- McConnaughey, T.A. and Whelan, J.F. 1997. Calcification generates protons for nutrient and bicarbonate uptake. *Earth Science Reviews* 42: 95–117.
- Mikkelsen, N., Erlenkauser, H., Killingley, J.S., and Berger, W.H. 1982. Norwegian corals: radiocarbon and stable isotopes in *Lophelia pertusa*. *Boreas* 5: 163–171.
- Montanaro-Gallitelli, E. 1975. Hexanthiniaria, a new ordo of Zoantharia (Anthozoa, Coelenterata). *Bollettino della Società Paleontologica Italiana* 14: 21–25.
- Mortensen, P.B. and Rapp, H.T. 1998. Oxygen and carbon isotope ratios related to growth line patterns in skeletons of *Lophelia pertusa* (L) (Anthozoa, Scleractinia): Implications for determination of linear extension rates. *Sarsia* 83: 433–446.
- Morycowa, E. and Roniewicz, E. 1990. Revision of the genus *Cladophyllia* and description of *Apocladophyllia* gen. n. (Cladophylliidae fam. n., Scleractinia). *Acta Palaeontologica Polonica* 29: 165–187.
- Ogilvie, M. 1897. Microscopic and systematic study of madreporarian types of corals. *Philosophical Transactions of the Royal Society of London* 187B: 83–345.
- Philippi, R.A. 1842. Zoologische Beobachtungen. 6. Verzeichniss der im Mittelmeer von mir beobachteten Arten *Cyathina* Ehrenberg. *Archiv für Naturgeschichte* 8: 40–44.
- Pourtales, L.F., de 1874. Zoological results of the Hassler expedition. Deep-sea corals. *Illustrated catalogue of the Museum of Comparative Zoology* [4] 8: 33–49.
- Pratz, E. 1882. Über die verwandtschaftlichen Beziehungen einiger Korallengattungen mit hauptsächlichlicher Berücksichtigung ihrer Septalstruktur. *Palaeontographica* 29: 81–122.
- Risk, M.J., Heikoop, J.M., Snow, M.G., and Beukens, R. 2002. Lifespans and growth patterns of two deep-sea corals: *Primnoa resedaeformis* and *Desmophyllum cristagalli*. *Hydrobiologia* 471: 125–131.
- Roberts, J.M. and Anderson, R.M. 2002. A new laboratory method for monitoring deep-water coral polyp behaviour. *Hydrobiologia* 471: 143–148.
- Romano, S.L. and Cairns, S.D. 2000. Molecular phylogenetic hypotheses for the evolution of scleractinian corals. *Bulletin of Marine Science* 67: 1043–1068.
- Roniewicz, E. 1989. Triassic scleractinian corals of the Zlambach Beds, Northern Calcareous Alps, Austria. *Oesterreichische Akademie der Wissenschaften, Mathematisch-Naturwissenschaftliche Klasse Denkschriften* 126: 1–152.
- Roniewicz, E. 1996. The key role of skeletal microstructure in recognizing high-rank scleractinian taxa in the stratigraphic record. *Palaeontological Society Papers* 1: 187–206.
- Roniewicz, E. and Morycowa, E. 1993. Evolution of the Scleractinia in the light of microstructural data. *Courier Forschungsinstitut Senckenberg* 164: 233–240.
- Roniewicz, E. and Stolarski, J. 1999. Evolutionary trends in the epithecate scleractinian corals. *Acta Palaeontologica Polonica* 44: 131–166.
- Roniewicz, E. and Stolarski, J. 2001. Triassic roots of the amphiastraeid scleractinian corals. *Journal of Paleontology* 75: 34–45.
- Schindewolf, O., von 1942. Zur Kenntnis der Polycoelien und Plerophyllen. Eine Studie über den Bau der "Tetrakorallen" und ihre Beziehungen zu

- den Madreporarien. *Abhandlungen des Reichsamts für Bodenforschung, N.F.* 204: 1–324.
- Schouppé, A., von and Stacul, P. 1955. Die genera *Verbeeliella* Penecke, *Timorphyllum* Gerth, *Wannerophyllum* n. gen., *Lophophyllidium* Grabau aus dem Perm von Timor. *Palaeontographica*, Supplement 4 (5): 95–196.
- Schouppé, A., von and Stacul, P. 1966. Morphogenese und Bau des Skelettes der Pterocorallia. *Palaeontographica*, Supplement 11: 1–186.
- Sorauf, J.E. 1972. Skeletal microstructure and microarchitecture in Scleractinia (Coelenterata). *Palaeontology* 15: 88–107.
- Sorauf, J.E. and Cuif, J.P. 2001. Biomineralization and diagenesis in Scleractinia: part II, diagenesis. *Bulletin of the Tohoku University Museum* 1: 152–163.
- Sorauf, J.E. and Freiwald, A. 2002. Skeletal structure in the rugosan genus *Calophyllum* from Permian strata of Timor: comparisons with the living deep water coral *Lophelia pertusa*. *Coral Research Bulletin* 7: 191–207.
- Sorauf, J.E. and Jell J.S. 1977. Structure and incremental growth in the ahermatypic coral *Desmophyllum cristagalli* from the North Atlantic. *Palaeontology* 20: 1–19.
- Sorauf, J.E. and Podoff, N. 1977. Skeletal structure in deep water ahermatypic corals. *Mémoires du Bureau de recherches géologiques et minières* 89: 2–11.
- Stolarski, J. 1990. On Cretaceous *Stephanocyathus* (Scleractinia) from the Tatra Mts. *Acta Palaeontologica Polonica* 35: 31–39.
- Stolarski, J. 1995. Ontogenetic development of the thecal structures in caryophylliine scleractinian corals. *Acta Paleontologica Polonica* 40: 19–44.
- Stolarski, J. 1999. Early ontogeny of the skeleton of Recent and fossil Scleractinia and its phylogenetic significance. *Abstracts of the VIII. International Symposium on Fossil Cnidaria including Archaeocyatha and Porifera. Sendai*, 37.
- Stolarski, J. 2000. Origin and phylogeny of Guyniidae (Scleractinia) in the light of microstructural data. *Lethaia* 33: 13–38.
- Stolarski, J. and Roniewicz, E. 2001. Towards a new synthesis of evolutionary relationships and classification of Scleractinia. *Journal of Paleontology* 75: 1090–1108.
- Stolarski, J. and Russo, A. 2001. Evolution of the post-Triassic pachythecaliine corals. *Bulletin of the Biological Society of Washington* 10: 242–256.
- Stolarski, J. and Russo, A. 2002. Microstructural diversity of the stylophyllid (Scleractinia) skeleton. *Acta Palaeontologica Polonica* 47: 651–666.
- Strömberg, T. 1987. The effect of light on the growth rate of intertidal *Acropora pulchra* from Phuket, Thailand, latitude 8 degrees North. *Coral Reefs* 6: 43–47.
- Teichert, C. 1958. Cold- and deep-water coral banks. *Bulletin of the American Association of Petroleum Geologists* 42: 1064–1082.
- Vaughan, T.W. and Wells, J.W. 1943. Revision of the suborders, families, and genera of the Scleractinia. *Geological Society of America, Special Paper* 44: 1–363.
- Veron, J.E.N. Odorico D.M. Chen C.A., and Miller D.J. 1996. Reassessing evolutionary relationships of scleractinian corals. *Coral Reefs* 15: 1–9.
- Wainwright, S.A. 1963. Skeletal organization in the coral, *Pocillopora damicornis*. *The Quarterly Journal of Microscopical Science* 104: 169–183.
- Waite, J.H. and Andersen, S.O. 1980. 3,4-Dihydroxyphenylalanine and the sclerotization of periostracum in *Mytilus edulis*. *Biological Bulletin* 158: 164–173.
- Watabe, N., Oishi, M., and Kingsley, R.J. 1991. The organic matrix of spicules of the gorgonian *Leptogorgia virgulata*. In: S. Suga and K. Nakahara (eds.), *Mechanisms and Phylogeny of Mineralization in Biological Systems*, 9–16. Springer-Verlag, Tokyo.
- Wells, J.W. 1956. Scleractinia. In: R.C. Moore (ed.), *Treatise on Invertebrate Paleontology, part F (Coelenterata)*, F328–F444. The University of Kansas Press, Lawrence, Kansas.
- Wells, J.W. 1963. Coral growth and geochronometry. *Nature* 197: 948–950.
- Wells, J.W. 1970. Problems of annual and daily growth-rings in corals. In: S.K. Runcorn (ed.), *Palaeogeophysics*, 3–9. Academic Press, London.
- Weyer, D. 1980. Zwei *Ufimia*-Arten aus dem Erdbacher Kalk im Rheinischen Schiefergebirge (Anthozoa, Rugosa; Unterkarbon). *Abhandlungen und Berichte für Naturkunde und Vorgeschichte* 12: 3–25.
- Wilson, J.B. 1979. “Patch” development of the deep-water coral *Lophelia pertusa* (L.) on Rockall Bank. *Journal of the Marine Biological Association of the United Kingdom* 59: 165–177.
- Wise, S.W. 1972. Observations of fasciculi on developmental surfaces of scleractinian coral exoskeletons. *Biomineralization, Research Reports* 6: 160–175.
- Wise, S.W., Stieglitz, R.D., and Hay, W.W. 1970. Scanning electron microscope study of fine grain size biogenic carbonate particles. *Gulf Coast Association of Geological Societies Transactions* 20: 287–302.
- Yamashiro, H. and Samata, T. 1996. New type of organic matrix in corals formed at the decalcified site: structure and composition. *Comparative Biochemistry and Physiology* 113A: 297–300.